

# FaVChat: Hierarchical Prompt-Query Guided Facial Video Understanding with Data-Efficient GRPO

Fufangchen Zhao<sup>1</sup> Songbai Tan<sup>2</sup> Xuerui Qiu<sup>3,4</sup> Linrui Xu<sup>5</sup> Wenhao Jiang<sup>2</sup> Jinkai Zheng<sup>6</sup> Hehe Fan<sup>7</sup>  
Jian Gao<sup>1</sup> Danfeng Yan<sup>1</sup> Ming Li<sup>2</sup>

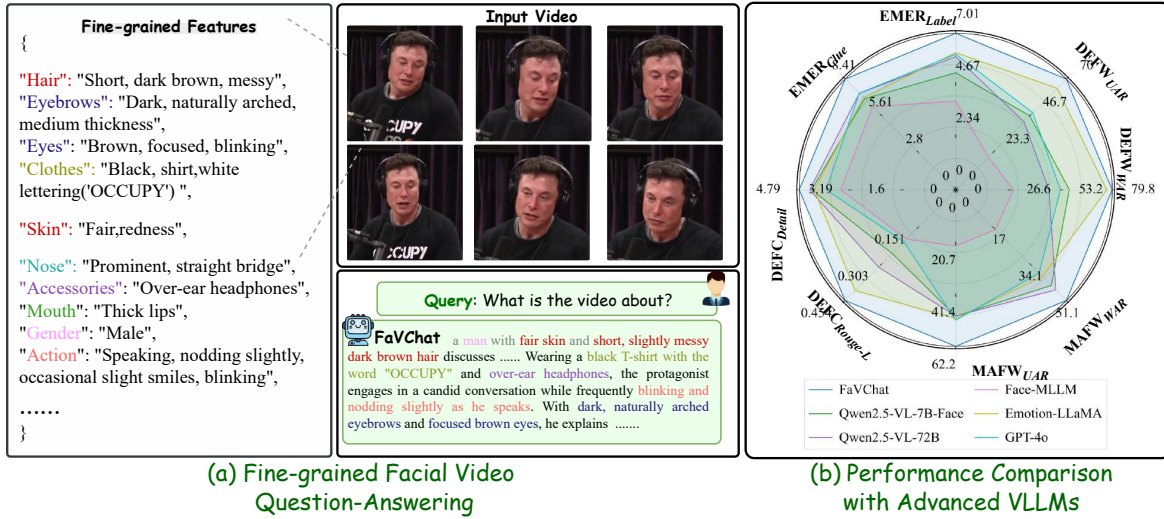


Figure 1. (a) The illustration of the proposed FaVChat for fine-grained facial video understanding. For input videos centered on human faces, FaVChat analyzes their fine-grained features based on the given prompts and provides fine-grained responses by integrating the analysis results with the posed questions. However, in the end-to-end user experience, the analysis results on the left side are not visible. (b) The Performance of FaVChat on different testsets.

## Abstract

Existing video large language models (VLLMs) primarily leverage *prompt-agnostic* visual encoders, which extract untargeted facial representations without awareness of the queried information, leading to the loss of task-critical cues. To address this challenge, we propose FaVChat, the *first* VLLM designed for reasoning over subtle visual and dynamic facial cues. FaVChat introduces a hierarchical, *prompt-guided* visual feature extraction framework that emphasizes question-relevant information at three complementary levels. These multi-level features are dynamically

fused and injected into the LLM, enabling more accurate facial details reasoning. To further improve learning efficiency under data scarcity, we propose Data-Efficient GRPO, a reinforcement learning strategy that iteratively identifies high-utility samples and maximizes the contribution of each instance via per-instance utility estimation, substantially enhancing performance gains under limited supervision. We construct a large-scale benchmark dataset, FaVChat-170K, comprising approximately 60K high-quality facial videos and 170K question-answer pairs focusing on fine-grained facial details. Extensive experiments, including zero-shot evaluations on four facial understanding tasks, demonstrate that FaVChat consistently outperforms existing VLLMs.

<sup>1</sup>State Key Laboratory of Networking and Switching Technology, BUCT <sup>2</sup>Guangdong Laboratory of Artificial Intelligence and Digital Economy (SZ) <sup>3</sup>Institute of automation, Chinese Academy of Sciences <sup>4</sup>Zhongguancun Academy <sup>5</sup>Central South University <sup>6</sup>College of communication Engineering, Hangzhou Dianzi University <sup>7</sup>Zhejiang University. Correspondence to: Fufangchen Zhao <zhaofufangchen@bupt.edu.cn>, Danfeng Yan <yandf@bupt.edu.cn>, Ming Li <ming.li@u.nus.edu>.

## 1. Introduction

By integrating visual encoders (Li et al., 2023a), large language models, and projection layers (Alayrac et al., 2022; Li et al., 2023a), multimodal large language models have

significantly advanced vision–language understanding and enabled cross-modal reasoning (Zhu et al., 2023b; Alayrac et al., 2022; Liu et al., 2023; Chen et al., 2024c). As video constitutes a primary medium for human perception and communication, video large language models (VLLMs) have emerged as a key frontier in multimodal research (Li et al., 2023b; Lin et al., 2023; Li et al., 2024b; Fei et al., 2024). Within this broader landscape, fine-grained facial video understanding plays a pivotal role, as it requires capturing subtle and localized facial cues—including skin texture, pupil characteristics, facial scars, and micro-level muscle movements—that are essential for real-world, human-centric intelligence (Lei et al., 2025; Zhao et al., 2025c; Yang et al., 2025b).

Despite this importance, existing VLLMs still face a fundamental challenge that limits their effectiveness in fine-grained facial understanding. Most current architectures rely on prompt-agnostic pure visual encoders, which extract representations without awareness of the queried information or task intent (Maaz et al., 2023; Luo et al., 2023; Jin et al., 2024; Li et al., 2024b). As a result, the learned visual features are coarse and untargeted, emphasizing generic semantics rather than question-relevant details. During hierarchical feature abstraction and evolution, subtle yet critical facial cues—such as fine textures, localized motions, and attribute-level variations—are consequently under-emphasized or discarded, hindering subsequent fine-grained comprehension in LLMs (Li et al., 2024b; Sun et al., 2024a).

Moreover, although reinforcement learning has recently shown promise for improving multimodal alignment, existing label-free reward optimization strategies rely predominantly on coarse preference signals (Deng et al., 2025b; Liu et al., 2025b; Yang et al., 2025c; Zhang et al., 2025). Such supervision is insufficient for guiding the modeling of dense and localized facial attributes (Guo et al., 2025). Consequently, effective reward design would require detailed annotations. However, collecting explicit fine-grained supervision remains prohibitively labor-intensive and difficult to scale.

To address these challenges, we present FaVChat, the first VLLM specifically designed for fine-grained facial video comprehension, as illustrated in Fig. 2. To overcome the limitation that query-relevant facial details are overlooked by prompt-agnostic visual encoders, FaVChat introduces a hierarchical prompt-guided visual feature extraction framework that progressively captures question-relevant information at three complementary levels: (1) low-level transformer features preserving fine textures and facial motions, (2) mid-level learnable queries attending to discriminative facial regions, and (3) high-level adaptive feature weighting for semantic alignment with language queries. These enriched

multi-level features are dynamically fused and injected into the LLM, enabling precise fine-grained understanding.

To further enable effective reinforcement learning under limited fine-grained supervision, we propose Data-Efficient (DE) GRPO, an iterative optimization strategy that estimates per-sample utility and dynamically schedules training to prioritize high-value samples. With only 10K training samples, DE-GRPO achieves significantly higher performance than the vanilla GRPO counterpart trained with substantially more data (170K as shown in Tab. 4). To support systematic training and evaluation, we devise a meticulous multi-step pipeline to construct a large-scale, high-quality cross-modal facial video dataset, FaVChat-170K, comprising over 60K carefully curated videos with rich captions and 170K question–answer (QA) pairs spanning 103 facial attributes, including appearance, actions, and emotions. Extensive experiments demonstrate that FaVChat achieves state-of-the-art performance on our benchmark as well as four zero-shot evaluation tasks. Notably, FaVChat (7B) outperforms Qwen2.5-VL-72B by 26.87 UAR and 32.27 WAR on the DFEW benchmark, despite using a substantially smaller model.

In summary, our main contributions are as follows:

- We present FaVChat, the first VLLM explicitly designed for fine-grained facial video comprehension, addressing a long-standing challenge in detailed facial analysis for multimodal understanding.
- We propose a hierarchical prompt-guided visual feature extraction framework that enables selective extraction of task-relevant cues while preserving subtle facial details for fine-grained reasoning.
- We introduce DE-GRPO, a data-efficient reinforcement learning algorithm that replaces coarse preference supervision with fine-grained optimization via per-sample utility estimation and dynamic lifecycle scheduling, substantially improving data efficiency under limited supervision.
- We contribute a large-scale, high-quality cross-modal facial video dataset, FaVChat-170K, comprising over 60K videos and 170K question–answer pairs covering 103 facial attributes across diverse appearances, actions, and emotions.

## 2. FaVChat

In this section, we present FaVChat, a MLLM framework designed for fine-grained facial video understanding. As illustrated in Fig. 2, FaVChat is built upon two tightly coupled components: a hierarchical prompt-query visual encoding that progressively preserves the fine-grained facial cues during visual encoding, and a data-efficient reinforcement learning strategy that enables effective fine-grained

alignment under limited data.

## 2.1. Hierarchical Prompt-Query Visual Encoding

**Motivation.** Existing video MLLMs usually encode visual inputs into a single set of text-agnostic embeddings, where textual prompts are only introduced at the final fusion stage. This design assumes that all task-relevant facial information has already been preserved during visual encoding. However, this design is insufficient in capturing the detailed facial features that are distributed across different spatial areas and network depths. We argue that fine-grained facial understanding requires textual prompts to guide visual encoding throughout the entire hierarchy, rather than being applied only after visual feature. Motivated by this, we decompose visual encoding into three prompt-query stages: (1) **low-level prompt-query learning** for retaining fine-grained facial cues, (2) **mid-level prompt-query learning** for extracting discriminative facial regions, and (3) **high-level prompt-query learning** for semantically adaptive fusion of visual features.

**Low-level Prompt-Query Learning.** As shown in Fig. 2, we utilize a dedicated facial encoder and a general vision encoder to extract facial fine-grained and general features, respectively. Within the facial encoder, we integrate a low-level prompt-query learning mechanism that enables textual queries to attend to intermediate spatiotemporal features, steering the aggregation of relevant details across Transformer layers. Specifically, the facial encoder processes an input video  $\mathbf{V} \in \mathbb{R}^{T \times C \times H \times W}$  through Transformer blocks, where the  $i$ -th block outputs features  $f_i(\mathbf{V}) \in \mathbb{R}^{T \times P_i \times D_i}$ , capturing information at different granularity. To facilitate cross-layer interaction, these features are projected into a shared embedding space:

$$\mathbf{W}_i = f_i(\mathbf{V})W_i, \quad \mathbf{W}_i \in \mathbb{R}^{T \times P_i \times D}. \quad (1)$$

Instead of relying solely on the final layer, we adopt a progressive prompt-query aggregation strategy based on a sequence of  $CA^2$  modules. In the first module, the textual embedding  $\mathbf{X}$  serves as the query to attend to the projected features  $\mathbf{W}_1$ :

$$Q_1 = \mathbf{X}W_Q, \quad K_1 = \mathbf{W}_1W_K, \quad V_1 = \mathbf{W}_1W_V. \quad (2)$$

For subsequent layers ( $i = 2, \dots, N$ ), we use the output of the preceding  $CA^2$  module as the query to attend to the current visual features:

$$Q_i = E_{i-1}, \quad K_i = \mathbf{W}_iW_K, \quad V_i = \mathbf{W}_iW_V, \quad (3)$$

$$E_i = \text{softmax} \left( \frac{Q_i K_i^\top}{\sqrt{d}} \right) V_i. \quad (4)$$

The final output  $E_N$  is taken as the facial fine-grained feature. Compared with directly adopting the final-layer feature, this approach better preserves subtle facial details from shallow layers while maintaining semantic alignment with the prompt-query.

**Medium-level Prompt-Query Learning.** Although low-level prompt-query learning preserves fine-grained cues, the resulting features remain dense and lack explicit semantic abstraction. Given the complementary inductive biases between the general vision encoder and the facial encoder, we introduce Q-Formers to extract discriminative mid-level representations. Each Q-Former uses learnable query tokens, guided by textual prompts, to selectively aggregate query-relevant visual information via cross-attention. This design converts dense visual features into compact, query-aligned tokens with distinct semantic roles, facilitating effective prompt-query guiding.

**High-level Prompt-Query Learning.** High-level prompt-query learning is designed to model the query-dependent importance of visual evidence derived from different encoders. Treating the general and facial streams as equally informative risks introducing irrelevant or redundant evidence. To address this issue, we introduce two text-conditioned weight adapters that estimate the contribution of the general and facial fine-grained features. Specifically, given visual tokens  $\mathbf{V}_g, \mathbf{V}_f \in \mathbb{R}^{L \times d}$  and the textual representation  $\mathbf{T} \in \mathbb{R}^{L \times d}$ , each adapter evaluates the alignment between its visual features and the input query, producing a scalar confidence score:

$$s_g = \mathcal{A}_g(\mathbf{V}_g, \mathbf{T}), \quad s_f = \mathcal{A}_f(\mathbf{V}_f, \mathbf{T}), \quad (5)$$

where  $\mathcal{A}_g(\cdot)$  and  $\mathcal{A}_f(\cdot)$  denote the general and fine-grained weight adapters, respectively. The resulting scores are normalized to obtain importance weights:

$$W_g = \frac{e^{s_g}}{e^{s_g} + e^{s_f}}, \quad W_f = \frac{e^{s_f}}{e^{s_g} + e^{s_f}}. \quad (6)$$

These weights dynamically regulate the contribution of each visual stream when conditioning the LLM, enabling adaptive emphasis on global structures or fine-grained details based on the query’s semantic intent.

## 2.2. Data Efficiency-GRPO

We propose Data-Efficient GRPO (DE-GRPO), which fundamentally departs from GRPO (Guo et al., 2025) and its derivatives (e.g., DrGRPO (Liu et al., 2025a), DAPO (Yu et al., 2025)) by redefining both reward granularity and data utility. First, to overcome the limitations of coarse preference signals in facial tasks, we introduce a facial-specific fine-grained reward that offers dense semantic guidance. Second, we propose a utility-aware recurrent data mechanism that fundamentally alters the optimization objective. As shown in Fig. 3, while GRPO computes group statistics to assess the quality of generated responses, DE-GRPO leverages these statistics to evaluate the utility of the input samples themselves. This shift allows DE-GRPO to act as a data quality probe, prioritizing informative samples and achieving higher data efficiency compared to the static data assumption used in standard GRPO approaches.

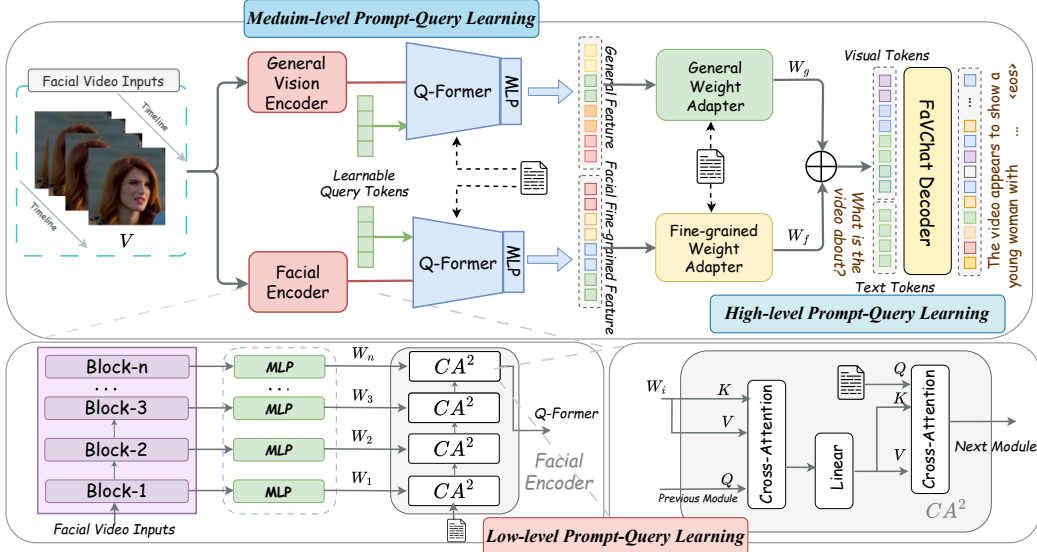


Figure 2. Overview of the proposed FaVChat framework. FaVChat augments the original visual encoder with an additional facial encoder (Narayan et al., 2024) and incorporates a multi-level prompt-guided feature extraction mechanism, comprising: (i) low-level prompt-query learning for progressive integration of Transformer features, (ii) mid-level prompt-query learning to support learnable queries, and (iii) high-level prompt-query learning to steer weight adaptation. This hierarchical prompting scheme enhances FaVChat’s sensitivity to fine-grained visual cues in videos and strengthens fine-grained alignment between video and textual representations.

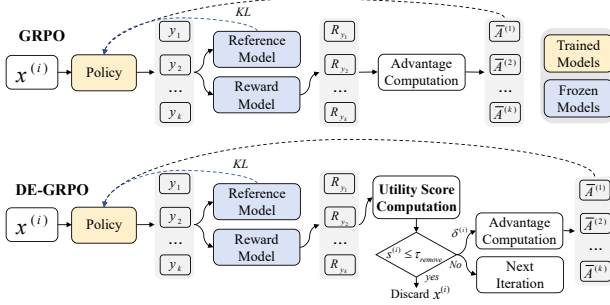


Figure 3. Concept diagrams of GRPO and DE-GRPO

**Facial-Specific Fine-Grained Reward.** Instead of relying solely on relative preference reward, we design a structured reward that explicitly evaluates fine-grained facial semantics, providing precise optimization signals than preference-only supervision. Given a generated response  $y_i$ , the reward is defined as

$$\mathbf{R}(y_i) = \sum_{j \in \{attr, emo, act\}} \alpha_j \cdot \text{Sim}(y_i, y_{i,j}^*), \quad (7)$$

where  $y_{i,j}^*$  denotes the ground-truth annotations for facial *attributes*, *emotions*, and *actions*, respectively.  $\text{Sim}(\cdot)$  measures semantic similarity, and  $\alpha_j$  are learnable weights normalized to  $\sum_j \alpha_j = 1$ .

**Recurrent Data Mechanism.** To maximize data efficiency, DE-GRPO introduces a recurrent mechanism that prioritizes training samples with high optimization utility. For each facial video sample  $x^{(i)}$ , the current policy  $\pi_\theta$  generates  $K$  ( $K \geq 4$ ) candidate responses, from which a set of preference pairs  $\mathcal{P}$  is constructed. These pairs serve as the

basis for utility estimation and policy optimization. The optimization utility of a training sample is evaluated along two dimensions. First, we measure reward separability  $\hat{R}^{(i)}$  to quantify how clearly the fine-grained reward distinguishes competing responses, with a larger value signifying a clearer supervision signal.

$$\hat{R}^{(i)} = \left\{ \prod_{(y_w, y_l) \in \mathcal{P}} \left| \mathbf{R}(y_w^{(i)}) - \mathbf{R}(y_l^{(i)}) \right| \right\}^{\frac{1}{|\mathcal{P}|}}, \quad (8)$$

where  $y_w$  and  $y_l$  denote the winning and losing responses in each pair, respectively. Second, we estimate gradient sensitivity  $\hat{g}^{(i)}$  to measure how differently the model parameters would be updated by generated responses.

$$\hat{g}^{(i)} = \left\{ \prod_{(y_w, y_l) \in \mathcal{P}} \left\| g(y_w^{(i)}) - g(y_l^{(i)}) \right\|_2 \right\}^{\frac{1}{|\mathcal{P}|}}, \quad (9)$$

where  $g(y^{(i)}) = \nabla_\theta \log \pi_\theta(y^{(i)} | x^{(i)})$ . A larger  $\hat{g}^{(i)}$  implies higher uncertainty and greater optimization potential. The overall utility score of the sample is defined as

$$U^{(i)} = \hat{R}^{(i)} \cdot \hat{g}^{(i)}. \quad (10)$$

To capture the long-term usefulness of each sample, we maintain a recurrent state variable  $s^{(i)}$  that is updated across training iterations using exponential smoothing:

$$s^{(i+1)} = \lambda \cdot s^{(i)} + (1 - \lambda) \cdot \mathbb{I}[U^{(i)} > \tau], \quad (11)$$

where  $i$  denotes the iteration step,  $\lambda$  controls temporal smoothing, and  $\tau$  is a batch-wise threshold. Based on  $s^{(i)}$ ,

the contribution of each sample is adaptively regulated. Samples with low  $s^{(i)}$  are removed, while high-utility ones are retained. To stabilize training and prevent overfitting to high-reward samples (Shumailov et al., 2024), we apply a reward decay (Kumar et al., 2010):

$$\delta^{(i)} = \begin{cases} \text{removed,} & s^{(i)} \leq \tau_{\text{remove}}, \\ \delta, & s^{(i)} \geq \tau_{\text{keep}}, \\ 1, & \text{otherwise.} \end{cases} \quad (12)$$

where  $\tau_{\text{remove}}$  and  $\tau_{\text{keep}}$  act as the lower and upper utility thresholds for filtering, respectively, and  $\delta \in (0, 1)$  is the decay factor. Finally, the policy is updated using the utility-weighted advantage:

$$\begin{aligned} \Delta R^{(i)} &= \frac{1}{|\mathcal{P}|} \sum_{(y_w, y_l) \in \mathcal{P}} \left( R(y_w^{(i)}) - R(y_l^{(i)}) \right), \\ \bar{A}^{(i)} &= \delta^{(i)} \cdot \left[ \Delta R^{(i)} - \mathbf{b}_\phi(x^{(i)}) \right], \end{aligned} \quad (13)$$

where  $\Delta R^{(i)}$  denotes the average fine-grained reward difference over  $\mathcal{P}$ , and  $\mathbf{b}_\phi(x^{(i)})$  is a learned value model that estimates the expected return of the input sample. This value model is trained jointly with the policy and serves as a critic to reduce variance and stabilize optimization. By dynamically regulating sample participation and influence at the data level, this recurrent mechanism enables DE-GRPO to concentrate gradient updates on informative facial supervision signals. More details of the overall objective function of DE-GRPO can see in App. D.

### 2.3. Progressive Pre-training Paradigm

As illustrate in Fig. 4, We adopt a progressive pre-training paradigm to support hierarchical prompt-query encoding. Firstly, we train the visual encoders and adapters on 60K video-summary pairs, freezing the Q-Formers and LLM to restrict guidance to low-level interactions and preserve subtle cues. Then, we switch to 170K video QA pairs and unfreeze the Q-Formers while keeping the adapters fixed, allowing prompt-guided query tokens to aggregate discriminative facial regions. Finally, we target high-level reasoning using 110K emotion-intensive QA pairs. Here, visual encoders remain frozen, while the adapters, Q-Formers, and LLM are trained to enable semantic query adaptation. This progressive strategy ensures that low-level details, mid-level discriminative regions, and high-level semantic relevance are learned in a structured manner.

## 3. Experiments

### 3.1. FaVChat-170K Dataset

To support fine-grained facial video understanding, we construct a large-scale dataset by curating and annotating videos from CelebV-HQ (Zhu et al., 2022), FERV39K (Wang et al.,

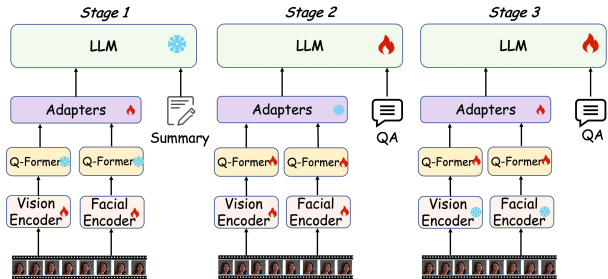


Figure 4. An illustration of our proposed pre-training paradigm.

2022), HMDB51 (Kuehne et al., 2011), and Youtube Faces (Wolf et al., 2011a), covering diverse identities, expressions, and actions. CelebV-HQ contains 35,666 clips across 15,653 subjects with 83 manually labeled facial attributes, while 25,341 additional videos from the other datasets provide varied facial motions. To compensate for missing textual annotations, we train a feature extraction module with three extractors to unify 103 fine-grained features per video, followed by GPT-4o (Hurst et al., 2024) to generate structured video summaries and QA pairs. This results in 60K high-quality video-summary pairs and 170K QA pairs, forming a comprehensive benchmark for fine-grained facial video understanding. As shown in Fig. 5, further dataset details are provided in App. B.

### 3.2. Quantitative Comparison

To demonstrate FaVChat’s advantages, we construct a 2,000-sample held-out test set from our internal dataset. These samples are excluded from training and annotated with detailed fine-grained labels and high-quality textual descriptions. We evaluate FaVChat and several baseline models on this test set using the VideoChatGPT score, extending the standard 5-point scale to 10 for more discriminative assessment. The corresponding experimental results are highlighted with \*.

The results, presented in Table 1, show that FaVChat consistently outperforms existing methods across nearly all metrics. Even in N-gram-based evaluations, where general models often struggle, FaVChat remains highly competitive. We attribute this to its ability to extract fine-grained facial features and subtle motion cues, leading to more contextually accurate and emotionally aligned predictions. These results highlight FaVChat’s strong capability in fine-grained facial video understanding, which is essential for precise emotion analysis.

### 3.3. Qualitative Comparison

Fig. 6 compares the facial video QA capabilities of FaVChat with several leading VLLMs. FaVChat generates the most detailed and expressive descriptions, capturing fine-grained facial attributes, skin texture, accessories, and subtle

Dataset	Video Resolution	VQA Availability	VQA pairs (Avg.)	Video	Caption Tokens (Avg.)	Attributes (Avg. per Caption)	Attributes Number (total)
HMDB51 (Wishart et al., 2022)	Low	✗	✗	6766	13.1	2.3	23
Youtube-face (Wolf et al., 2011b)		✗	✗	3425	✗	✗	11
FERV39K (Wang et al., 2022)	High	✗	✗	39546	11.3	1.3	7
CelebV-HQ (Zhu et al., 2022)		✗	✗	35666	✗	✗	83
<b>FaVChat-170K</b>		✓(170K)	✓(2.8)	61007	100.7	23.4	103

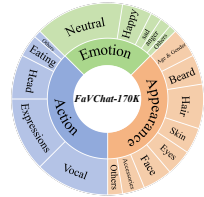


Figure 5. Comparison results between FaVChat-170K and other mainstream face video datasets, our FaVChat contains the largest number of videos and the richest set of attribute categories. To the best of our knowledge, it is also the first face video dataset designed for VQA training.

Table 1. Performance comparison on the DFEC (Zhao et al., 2025a) dataset for textual emotion analysis. The \* columns show VideoChatGPT Scores (0–10) evaluated on our internally curated test dataset. ♣ denotes a model trained to process both visual and speech modalities. ”-Face” denotes the variant fine-tuned on our FaVChat-170K dataset. This table includes only results from recent high-performing models. The complete results are provided in App. F.

Method	LLM	VideoChatGPT Scores					N-gram Based		Event Based
		Size	Test(2000)*	Correctness	Detail	Context	Temporal	CIDEr	Rouge-L
<i>General VLLM</i>									
ShareGPT4Video (Chen et al., 2024b)	7B	7.33	4.24	4.13	4.35	4.09	0.192	0.205	0.394
VideoLLaMA2 (Cheng et al., 2024)	7B	7.41	4.17	4.02	4.47	3.93	0.253	0.266	0.344
PLLaVA (Xu et al., 2024)	7B	7.47	4.21	4.15	4.37	4.08	0.268	0.250	0.393
Qwen2.5-VL-7B (Bai et al., 2025b)	7B	7.84	4.49	4.36	4.43	4.21	0.261	0.254	0.417
Qwen2.5-VL-72B (Bai et al., 2025b)	72B	8.47	4.61	4.47	4.59	4.78	0.281	0.317	0.453
Qwen3-VL-8B (Bai et al., 2025a)	8B	7.99	4.49	4.37	4.41	4.33	0.262	0.257	0.421
Qwen3-VL-30B-A3B (Bai et al., 2025a)	30B	8.44	4.63	4.51	4.57	4.81	0.304	0.331	0.461
Claude4-Sonnet (Anthropic, 2025)	-	7.84	4.55	4.64	4.77	4.84	0.312	0.342	0.472
GPT-4o (OpenAI, 2024)	-	7.67	4.22	3.97	4.48	3.90	0.264	0.213	0.432
<i>Human-Centric VLLM</i>									
FaceTrack-MM (Zhao et al., 2025a)	7B	7.47	4.42	4.30	4.60	4.26	0.418	0.473	0.483
Qwen2.5-VL-7B-Face (Bai et al., 2025b)	7B	8.64	4.51	4.41	4.45	4.22	0.274	0.261	0.463
Qwen3-VL-8B-Face (Bai et al., 2025a)	8B	8.87	4.58	4.46	4.47	4.51	0.297	0.312	0.429
Emotion-LLaMA♣ (Cheng et al., 2025)	7B	7.42	4.17	4.33	4.54	4.19	0.294	0.413	0.372
HumanOmni♣ (Zhao et al., 2025c)	7B	7.51	4.58	4.41	4.70	4.41	0.412	0.468	<b>0.523</b>
Omni-Emotion♣ (Yang et al., 2025b)	7B	7.53	4.57	4.38	4.73	4.24	0.407	0.461	0.504
<b>FaVChat</b> <sub>Qwen2.5</sub>	7B	8.89	4.84	4.79	4.69	4.78	0.443	0.454	0.487
<b>FaVChat</b> <sub>Qwen3</sub>	8B	<b>9.01</b>	<b>4.87</b>	<b>4.82</b>	<b>4.74</b>	<b>4.81</b>	<b>0.447</b>	<b>0.469</b>	<b>0.523</b>

expression changes (e.g., “downward-angled head, rounded shoulders, nods, slight smile, narrowed eyes”). In contrast, models such as Qwen3-vl-8B-Face (Bai et al., 2025a), GPT-4o (Hurst et al., 2024), and Qwen3-vl-30B-A3B (Bai et al., 2025a) focus mainly on general appearance, clothing, and background, missing many facial details and dynamic cues. These results demonstrate FaVChat’s strong fine-grained facial understanding, making it well suited for tasks such as emotion recognition and human–computer interaction.

### 3.4. Zero-shot Generalizations

**Textual Facial Analysis.** Facial expressions reflect internal emotional states such as happiness, sadness, or anger through subtle movements like smiling, frowning, or smirking. Yet a single expression can map to multiple emotions, making facial emotion analysis inherently ambiguous. Accurate recognition therefore requires fine-grained feature extraction and precise motion modeling. Given FaVChat’s strength in capturing subtle facial dynamics, we evaluate its effectiveness on this task using the recently released DFEC dataset (Zhao et al., 2025a) and its recommended metrics. As shown in Tab. 1, we conducted supplementary

evaluations of FaVChat using Qwen3 (Yang et al., 2025a) as the backbone model. Notably, to ensure a fair comparison, all results presented in other generalizations are derived from FaVChat evaluations with Qwen2.5-base (Team, 2024) serving as the backbone.

**Emotion Classification.** In this section, we evaluate FaVChat on emotion recognition using two large-scale in-the-wild datasets: DFEW (Jiang et al., 2020) and MAFW (Liu et al., 2022), both designed for dynamic facial expression analysis. DFEW provides a seven-dimensional emotion distribution, while MAFW offers an eleven dimensional distribution.

To make full use of FaVChat’s capabilities, we first prompt FaVChat to generate fine-grained descriptions for each video clip, and then instruct it to infer emotions from these detailed descriptions, enabling more context-aware predictions. As shown in Table 2, even when using only visual inputs, FaVChat outperforms all existing methods, including models that combine video and audio. This demonstrates the effectiveness of fine-grained descriptions in improving facial emotion recognition. Other zero-shot results are provided in App. I.

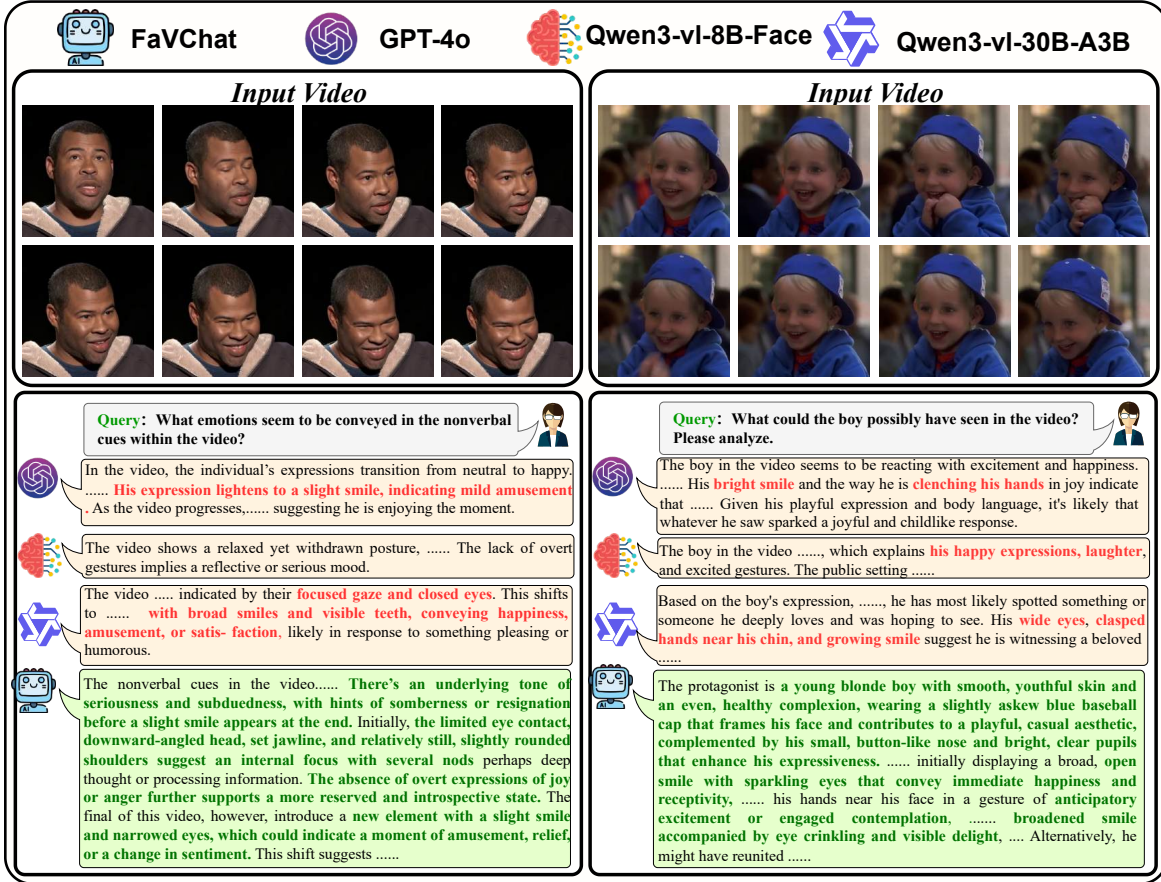


Figure 6. Qualitative comparison of facial video question-answering capabilities among FaVChat and other high-performance VLLMs. Given the same user prompt, FaVChat provides the most detailed and fine-grained description, capturing intricate facial attributes, expressions, and dynamic movements, while other models focus more on general appearance and background details. This highlights FaVChat’s superior ability in fine-grained facial video understanding.

Table 2. Comparison with existing methods on two large in-the-wild emotion classification datasets.

Dataset	DFEW (Jiang et al., 2020) MAFW(Liu et al., 2022)				
	modality	UAR	WAR	UAR	WAR
TMEP (Zhang et al., 2023b)	AV	57.16	68.85	37.17	51.15
HiCMAE (Sun et al., 2024c)	AV	63.76	75.01	42.65	56.17
Emotion-LLaMA (Cheng et al., 2025)	AV	64.21	77.06	-	-
MMA-DFER (Chumachenko et al., 2024)	AV	66.01	77.51	44.11	58.52
DFER-CLIP (Zhao & Patras, 2023)	V	59.61	71.25	38.89	52.55
SVFAP (Sun et al., 2024d)	V	62.83	74.27	41.19	54.28
MAE-DFER (Sun et al., 2023a)	V	63.41	74.43	41.62	54.31
Finecliper (Chen et al., 2024a)	V	65.98	76.21	45.01	56.91
Qwen2.5-VL-7B-Face (Bai et al., 2025b)	V	46.78	57.93	44.13	50.17
Qwen2.5-VL-72B (Bai et al., 2025b)	V	43.14	47.52	46.18	50.11
<b>FaVChat</b>	V	<b>70.01</b>	<b>79.79</b>	<b>51.09</b>	<b>62.17</b>

### 3.5. Ablation Study

**Key Components in FaVChat.** To analyze the contributions of key components in FaVChat, we conduct ablation experiments on main model variants.

- Without Facial Encoder (w/o FE): We remove the facial encoder and apply the multi-granularity strategy to the general visual encoder, evaluating the necessity of incorporating a dedicated facial encoder.
- Without  $CA^2$  module (w/o  $CA^2$ ): We replace the  $CA^2$

Table 3. Ablation study results on the impact of key components in FaVChat.

Models	DFEW-WAR	MAFW-WAR
FaVChat	<b>79.79</b>	<b>62.17</b>
FaVChat w/o FE	55.01	55.01
FaVChat w/o $CA^2$	70.04	57.49
FaVChat w/o Adapters	72.53	58.31

module with a standard cross-attention module to assess the contribution of our  $CA^2$ -based multi-granularity learning approach.

- Without Weight Adapters: (w/o Adapters): To verify the effectiveness of the Weight Adapters, we conducted experiments by removing the introduced MoE Adapter component and replacing it with a simple vector weighted summation.

We evaluate these variants on DFEW (Jiang et al., 2020) and MAFW (Liu et al., 2022), using the WAR metric as a performance indicator. The results in Table 3 show that removing either module leads to a notable performance drop, confirming that both the facial encoder and multi-granularity strategy play essential roles in enhancing fine-grained facial

Table 4. Ablation study results on the impact of data-efficient reinforcement learning in FaVChat

Method	LLM Size	VideoChatGPT Scores				N-gram Based		Event Based
		Correctness	Detail	Context	Temporal	CIDEr	Rouge-L	AutoDQ
FaVChat <sub>w.o.</sub> RL	7B	4.67	4.48	4.51	4.56	0.432	0.447	0.464
FaVChat <sub>w.</sub> GRPO	7B	4.68	4.48	4.52	4.54	0.433	0.449	0.461
FaVChat <sub>w.</sub> GRPO(170K)	7B	4.71	4.54	4.59	4.74	0.434	0.452	0.473
FaVChat <sub>w.o.</sub> RD	7B	4.73	4.67	4.57	4.64	0.437	0.451	0.477
<b>FaVChat<sub>DE-GRPO</sub></b>	7B	<b>4.84</b>	<b>4.79</b>	<b>4.69</b>	<b>4.78</b>	<b>0.443</b>	<b>0.454</b>	<b>0.487</b>

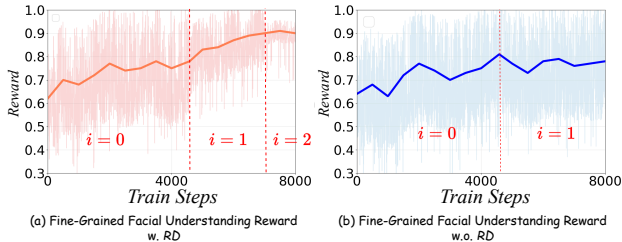


Figure 7. The performance of Facial-Specific Fine-Grained Reward in data recurrent mechanism ablation, where  $i$  represents the number of iterations of the training.

video understanding.

**Data-Efficient GRPO.** To demonstrate the effectiveness of the proposed DE-GRPO, we performed the following ablation studies on the model during the reinforcement learning phase:

- Without Reinforcement Learning (w.o. RL): We omit all reinforcement learning training steps and directly evaluate the model’s performance after fine-tuning to assess the necessity of RL stage.
- With Standard GRPO (w. GRPO): We train the model using standard GRPO rewards (e.g., output format and length) to evaluate the effectiveness of our reward mechanism. Furthermore, we incorporate the entire FaVChat-170K training dataset into the GRPO training process to assess the data efficiency of our DE-GRPO method.
- Without Recurrent Data Mechanism (w.o. RD): We exclude the data recurrent mechanism. After the first training round, we directly feed all data into the second round, ensuring that the total number of training steps matches that of the main experiment, evaluating the effectiveness of the data recurrent mechanism.

We evaluate the aforementioned variants on the DFEC dataset. As shown in Table 4, removing any component of the reinforcement learning framework results in a significant performance degradation. To assess the impact of the data recurrent mechanism, we visualize the fine-grained facial understanding reward curves with and without this mechanism in Figure 7. The results show that, when the data mechanism is employed, the reward steadily improves across multiple training rounds; in contrast, without this

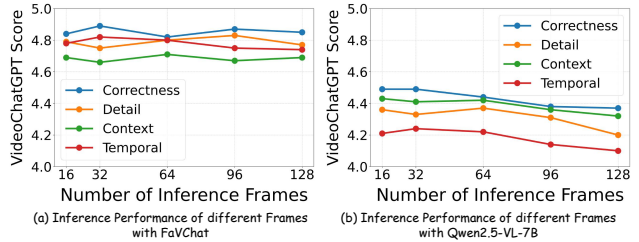


Figure 8. Influence of different inference frames length.

mechanism, the reward exhibits little to no improvement after the first round. These findings demonstrate the substantial contribution of our proposed DE-GRPO framework, which incorporates the data recurrent mechanism.

**Influence of Inference Frame Length.** We evaluate the effect of varying input frame counts during inference on both FaVChat and Qwen2.5-VL-7B (Bai et al., 2025b), using the VideoChatGPT scores on the DFEC benchmark (Zhao et al., 2025a) as the evaluation metric. As shown in Fig. 8, FaVChat maintains stable performance as the number of input frames increases, whereas Qwen2.5-VL-7B shows a noticeable decline when the input exceeds 96 frames. This demonstrates that FaVChat effectively preserves fine-grained information even in long videos, providing a strong basis for our subsequent work on long-video understanding.

## 4. Conclusion

In this work, we proposed FaVChat, a novel multi-modal large language model tailored for fine-grained facial video understanding. By introducing a hierarchical prompt-query guided feature extraction mechanism and a data-efficient reinforcement learning framework (DE-GRPO), FaVChat effectively captures subtle facial cues and optimizes learning with limited data. Extensive experiments demonstrated its superior performance in tasks such as emotion recognition, explainable reasoning, and facial analysis. The results highlight FaVChat’s ability to preserve fine-grained details and generalize well with minimal supervision. Future work will explore extending this approach to other fine-grained video domains and further improving data efficiency for large-scale applications.

## 5. Impact Statement

FaVChat enables precise facial video understanding by capturing subtle visual and dynamic cues such as micro-expressions, fine-grained textures, and facial motions. This capability supports human-centric applications including mental health assessment, empathetic and socially aware AI, and behavioral research, where nuanced facial signals are essential. By releasing the FaVChat-170K dataset and the data-efficient DE-GRPO framework, this work promotes reproducible research and lowers the barrier to fine-grained facial understanding, ultimately contributing to the development of assistive AI systems that augment human judgment and enhance human-machine interaction.

## References

- Alayrac, J.-B., Donahue, J., Luc, P., Miech, A., Barr, I., Hasson, Y., Lenc, K., Mensch, A., Millican, K., Reynolds, M., et al. Flamingo: a visual language model for few-shot learning. *Advances in neural information processing systems*, 35:23716–23736, 2022.
- Anthropic. Claude-4, 2025. URL <https://www.anthropic.com/news/claude-4>.
- Bai, S., Cai, Y., Chen, R., Chen, K., Chen, X., Cheng, Z., Deng, L., Ding, W., Gao, C., Ge, C., Ge, W., Guo, Z., Huang, Q., Huang, J., Huang, F., Hui, B., Jiang, S., Li, Z., Li, M., Li, M., Li, K., Lin, Z., Lin, J., Liu, X., Liu, J., Liu, C., Liu, Y., Liu, D., Liu, S., Lu, D., Luo, R., Lv, C., Men, R., Meng, L., Ren, X., Ren, X., Song, S., Sun, Y., Tang, J., Tu, J., Wan, J., Wang, P., Wang, P., Wang, Q., Wang, Y., Xie, T., Xu, Y., Xu, H., Xu, J., Yang, Z., Yang, M., Yang, J., Yang, A., Yu, B., Zhang, F., Zhang, H., Zhang, X., Zheng, B., Zhong, H., Zhou, J., Zhou, F., Zhou, J., Zhu, Y., and Zhu, K. Qwen3-vl technical report, 2025a. URL <https://arxiv.org/abs/2511.21631>.
- Bai, S., Chen, K., Liu, X., Wang, J., Ge, W., Song, S., Dang, K., Wang, P., Wang, S., Tang, J., Zhong, H., Zhu, Y., Yang, M., Li, Z., Wan, J., Wang, P., Ding, W., Fu, Z., Xu, Y., Ye, J., Zhang, X., Xie, T., Cheng, Z., Zhang, H., Yang, Z., Xu, H., and Lin, J. Qwen2.5-vl technical report. *arXiv preprint arXiv:2502.13923*, 2025b.
- Cao, W., Mirjalili, V., and Raschka, S. Rank consistent ordinal regression for neural networks with application to age estimation. *Pattern Recognition Letters*, 140:325–331, 2020.
- Chang, T., Wen, G., Hu, Y., and Ma, J. Facial expression recognition based on complexity perception classification algorithm. *arXiv preprint arXiv:1803.00185*, 2018.
- Chen, H., Huang, H., Dong, J., Zheng, M., and Shao, D. Finecliper: Multi-modal fine-grained clip for dynamic facial expression recognition with adapters. In *Proceedings of the 32nd ACM International Conference on Multimedia*, pp. 2301–2310, 2024a.
- Chen, L., Wei, X., Li, J., Dong, X., Zhang, P., Zang, Y., Chen, Z., Duan, H., Tang, Z., Yuan, L., et al. Sharegpt4video: Improving video understanding and generation with better captions. *Advances in Neural Information Processing Systems*, 37:19472–19495, 2024b.
- Chen, Z., Wu, J., Wang, W., Su, W., Chen, G., Xing, S., Zhong, M., Zhang, Q., Zhu, X., Lu, L., et al. Internvl: Scaling up vision foundation models and aligning for generic visual-linguistic tasks. In *Proceedings of the IEEE/CVF conference on computer vision and pattern recognition*, pp. 24185–24198, 2024c.
- Cheng, Z., Leng, S., Zhang, H., Xin, Y., Li, X., Chen, G., Zhu, Y., Zhang, W., Luo, Z., Zhao, D., et al. Videollama 2: Advancing spatial-temporal modeling and audio understanding in video-llms. *arXiv preprint arXiv:2406.07476*, 2024.
- Cheng, Z., Cheng, Z.-Q., He, J.-Y., Wang, K., Lin, Y., Lian, Z., Peng, X., and Hauptmann, A. Emotion-llama: Multimodal emotion recognition and reasoning with instruction tuning. *Advances in Neural Information Processing Systems*, 37:110805–110853, 2025.
- Chumachenko, K., Iosifidis, A., and Gabbouj, M. Mma-dfer: Multimodal adaptation of unimodal models for dynamic facial expression recognition in-the-wild. In *Proceedings of the IEEE/CVF Conference on Computer Vision and Pattern Recognition*, pp. 4673–4682, 2024.
- Cobo, A., Valle, R., Buenaposada, J. M., and Baumela, L. On the representation and methodology for wide and short range head pose estimation. *Pattern Recognition*, pp. 110263, May 2024. doi: 10.1016/j.patcog.2024.110263. URL <http://dx.doi.org/10.1016/j.patcog.2024.110263>.
- Deng, H., Zou, D., Ma, R., Luo, H., Cao, Y., and Kang, Y. Boosting the generalization and reasoning of vision language models with curriculum reinforcement learning. *arXiv preprint arXiv:2503.07065*, 2025a.
- Deng, Y., Bansal, H., Yin, F., Peng, N., Wang, W., and Chang, K.-W. Openvlthinker: An early exploration to complex vision-language reasoning via iterative self-improvement. *arXiv preprint arXiv:2503.17352*, 2025b.
- Fei, J., Li, D., Deng, Z., Wang, Z., Liu, G., and Wang, H. Video-ccam: Enhancing video-language understanding with causal cross-attention masks for short and long videos. *arXiv preprint arXiv:2408.14023*, 2024.

- Feng, K., Gong, K., Li, B., Guo, Z., Wang, Y., Peng, T., Wu, J., Zhang, X., Wang, B., and Yue, X. Video-r1: Reinforcing video reasoning in mllms. *arXiv preprint arXiv:2503.21776*, 2025.
- Guo, D., Yang, D., Zhang, H., Song, J., Zhang, R., Xu, R., Zhu, Q., Ma, S., Wang, P., Bi, X., et al. Deepseek-r1: Incentivizing reasoning capability in llms via reinforcement learning. *arXiv preprint arXiv:2501.12948*, 2025.
- Hurst, A., Lerer, A., Goucher, A. P., Perelman, A., Ramesh, A., Clark, A., Ostrow, A., Welihinda, A., Hayes, A., Radford, A., et al. Gpt-4o system card. *arXiv preprint arXiv:2410.21276*, 2024.
- Jiang, X., Zong, Y., Zheng, W., Tang, C., Xia, W., Lu, C., and Liu, J. Dfew: A large-scale database for recognizing dynamic facial expressions in the wild. In *Proceedings of the 28th ACM international conference on multimedia*, pp. 2881–2889, 2020.
- Jin, P., Takanobu, R., Zhang, W., Cao, X., and Yuan, L. Chat-univi: Unified visual representation empowers large language models with image and video understanding. In *Proceedings of the IEEE/CVF Conference on Computer Vision and Pattern Recognition*, pp. 13700–13710, 2024.
- Kuehne, H., Jhuang, H., Garrote, E., Poggio, T., and Serre, T. Hmdb: a large video database for human motion recognition. In *2011 International conference on computer vision*, pp. 2556–2563. IEEE, 2011.
- Kumar, M., Packer, B., and Koller, D. Self-paced learning for latent variable models. *Advances in neural information processing systems*, 23, 2010.
- Kuprashevich, M. and Tolstykh, I. Mivolo: Multi-input transformer for age and gender estimation. In *International Conference on Analysis of Images, Social Networks and Texts*, pp. 212–226. Springer, 2023.
- Lei, C., Dang, K., Song, S., Wang, Z., Chew, S. P., Bian, R., Yang, X., Guan, Z., de Abreu Lopes, C. I. M., Wang, M. H., et al. Ai-assisted facial analysis in healthcare: From disease detection to comprehensive management. *Patterns*, 2025.
- Li, B., Zhang, Y., Guo, D., Zhang, R., Li, F., Zhang, H., Zhang, K., Zhang, P., Li, Y., Liu, Z., et al. Llava-onevision: Easy visual task transfer. *arXiv preprint arXiv:2408.03326*, 2024a.
- Li, J., Li, D., Savarese, S., and Hoi, S. Blip-2: Bootstrapping language-image pre-training with frozen image encoders and large language models. In *International conference on machine learning*, pp. 19730–19742. PMLR, 2023a.
- Li, K., He, Y., Wang, Y., Li, Y., Wang, W., Luo, P., Wang, Y., Wang, L., and Qiao, Y. Videochat: Chat-centric video understanding. *arXiv preprint arXiv:2305.06355*, 2023b.
- Li, K., Wang, Y., Li, Y., Wang, Y., He, Y., Wang, L., and Qiao, Y. Unmasked teacher: Towards training-efficient video foundation models. In *Proceedings of the IEEE/CVF International Conference on Computer Vision*, pp. 19948–19960, 2023c.
- Li, K., Wang, Y., He, Y., Li, Y., Wang, Y., Liu, Y., Wang, Z., Xu, J., Chen, G., Luo, P., et al. Mvbench: A comprehensive multi-modal video understanding benchmark. In *Proceedings of the IEEE/CVF Conference on Computer Vision and Pattern Recognition*, pp. 22195–22206, 2024b.
- Li, S. and Deng, W. Deep facial expression recognition: A survey. *IEEE transactions on affective computing*, 13(3): 1195–1215, 2020.
- Li, Y., Wang, C., and Jia, J. Llama-vid: An image is worth 2 tokens in large language models. In *European Conference on Computer Vision*, pp. 323–340. Springer, 2024c.
- Lian, Z., Sun, L., Xu, M., Sun, H., Xu, K., Wen, Z., Chen, S., Liu, B., and Tao, J. Explainable multimodal emotion reasoning. *CoRR*, 2023.
- Lin, B., Ye, Y., Zhu, B., Cui, J., Ning, M., Jin, P., and Yuan, L. Video-llava: Learning united visual representation by alignment before projection. *arXiv preprint arXiv:2311.10122*, 2023.
- Liu, H., Li, C., Wu, Q., and Lee, Y. J. Visual instruction tuning. *Advances in neural information processing systems*, 36:34892–34916, 2023.
- Liu, R., Li, C., Tang, H., Ge, Y., Shan, Y., and Li, G. St-llm: Large language models are effective temporal learners. In *European Conference on Computer Vision*, pp. 1–18. Springer, 2024.
- Liu, Y., Dai, W., Feng, C., Wang, W., Yin, G., Zeng, J., and Shan, S. Mafw: A large-scale, multi-modal, compound affective database for dynamic facial expression recognition in the wild. In *Proceedings of the 30th ACM international conference on multimedia*, pp. 24–32, 2022.
- Liu, Z., Chen, C., Li, W., Qi, P., Pang, T., Du, C., Lee, W. S., and Lin, M. Understanding r1-zero-like training: A critical perspective. *arXiv preprint arXiv:2503.20783*, 2025a.
- Liu, Z., Sun, Z., Zang, Y., Dong, X., Cao, Y., Duan, H., Lin, D., and Wang, J. Visual-rft: Visual reinforcement fine-tuning. *arXiv preprint arXiv:2503.01785*, 2025b.

- Long, M., Cao, Y., Wang, J., and Jordan, M. Learning transferable features with deep adaptation networks. In *International conference on machine learning*, pp. 97–105. PMLR, 2015.
- Luo, R., Zhao, Z., Yang, M., Dong, J., Li, D., Lu, P., Wang, T., Hu, L., Qiu, M., and Wei, Z. Valley: Video assistant with large language model enhanced ability. *arXiv preprint arXiv:2306.07207*, 2023.
- Ma, F., Jin, X., Wang, H., Xian, Y., Feng, J., and Yang, Y. Vista-llama: Reliable video narrator via equal distance to visual tokens. *arXiv preprint arXiv:2312.08870*, 2023.
- Maaz, M., Rasheed, H., Khan, S., and Khan, F. S. Video-chatgpt: Towards detailed video understanding via large vision and language models. *arXiv preprint arXiv:2306.05424*, 2023.
- Narayan, K., VS, V., Chellappa, R., and Patel, V. M. Facexformer: A unified transformer for facial analysis. *arXiv preprint arXiv:2403.12960*, 2024.
- OpenAI. Gpt-4o system card, 2024. URL <https://openai.com/index/hello-gpt-4o/>.
- Qi, L., Chen, X., Wang, Y., Wang, K., Zhao, H., et al. Star-r1: Improving video perception via spatio-temporal aggregated reinforcement. In *The Thirty-ninth Annual Conference on Neural Information Processing Systems*.
- Qin, L., Wang, M., Deng, C., Wang, K., Chen, X., Hu, J., and Deng, W. Swinface: A multi-task transformer for face recognition, expression recognition, age estimation and attribute estimation. *IEEE Transactions on Circuits and Systems for Video Technology*, 34(4):2223–2234, 2023.
- Qin, L., Wang, M., Liu, X., Zhang, Y., Deng, W., Song, X., Xu, W., and Deng, W. Faceptor: A generalist model for face perception. In *European Conference on Computer Vision*, pp. 240–260. Springer, 2024.
- Ranjan, R., Sankaranarayanan, S., Castillo, C., and Chellappa, R. An all-in-one convolutional neural network for face analysis. *Cornell University - arXiv, Cornell University - arXiv*, Nov 2016.
- Ranjan, R., Patel, V. M., and Chellappa, R. Hyperface: A deep multi-task learning framework for face detection, landmark localization, pose estimation, and gender recognition. *IEEE Transactions on Pattern Analysis and Machine Intelligence*, pp. 121–135, Jan 2019. doi: 10.1109/tpami.2017.2781233. URL <http://dx.doi.org/10.1109/tpami.2017.2781233>.
- Ren, S., Yao, L., Li, S., Sun, X., and Hou, L. Timechat: A time-sensitive multimodal large language model for long video understanding. In *Proceedings of the IEEE/CVF Conference on Computer Vision and Pattern Recognition*, pp. 14313–14323, 2024.
- Ren, X., Lattas, A., Gecer, B., Deng, J., Ma, C., and Yang, X. Facial geometric detail recovery via implicit representation. In *2023 IEEE 17th International Conference on Automatic Face and Gesture Recognition (FG)*, 2023.
- Shao, Z., Wang, P., Zhu, Q., Xu, R., Song, J., Bi, X., Zhang, H., Zhang, M., Li, Y., Wu, Y., et al. Deepseekmath: Pushing the limits of mathematical reasoning in open language models. *arXiv preprint arXiv:2402.03300*, 2024.
- Shu, Y., Yan, Y., Chen, S., Xue, J.-H., Shen, C., and Wang, H. Learning spatial-semantic relationship for facial attribute recognition with limited labeled data. In *2021 IEEE/CVF Conference on Computer Vision and Pattern Recognition (CVPR)*, Jun 2021. doi: 10.1109/cvpr46437.2021.01174. URL <http://dx.doi.org/10.1109/cvpr46437.2021.01174>.
- Shumailov, I., Shumaylov, Z., Zhao, Y., Papernot, N., Anderson, R., and Gal, Y. Ai models collapse when trained on recursively generated data. *Nature*, 631(8022):755–759, 2024.
- Su, Y., Lan, T., Li, H., Xu, J., Wang, Y., and Cai, D. Pandagpt: One model to instruction-follow them all. *arXiv preprint arXiv:2305.16355*, 2023.
- Sun, H., He, M., Lian, T., Han, H., and Shan, S. Face-mlm: A large face perception model. *arXiv preprint arXiv:2410.20717*, 2024a.
- Sun, H., He, M., Shan, S., Han, H., and Chen, X. Task-adaptive q-face. *arXiv preprint arXiv:2405.09059*, 2024b.
- Sun, L., Lian, Z., Liu, B., and Tao, J. Mae-dfer: Efficient masked autoencoder for self-supervised dynamic facial expression recognition. In *Proceedings of the 31st ACM International Conference on Multimedia*, pp. 6110–6121, 2023a.
- Sun, L., Lian, Z., Liu, B., and Tao, J. Hicmae: Hierarchical contrastive masked autoencoder for self-supervised audiovisual emotion recognition. *Information Fusion*, 108: 102382, 2024c.
- Sun, L., Lian, Z., Wang, K., He, Y., Xu, M., Sun, H., Liu, B., and Tao, J. Svfap: Self-supervised video facial affect perceiver. *IEEE Transactions on Affective Computing*, 2024d.
- Sun, Q., Fang, Y., Wu, L., Wang, X., and Cao, Y. Evalclip: Improved training techniques for clip at scale. *arXiv preprint arXiv:2303.15389*, 2023b.

- Te, G., Liu, Y., Hu, W., Shi, H., and Mei, T. Edge-aware graph representation learning and reasoning for face parsing. In *Computer Vision—ECCV 2020: 16th European Conference, Glasgow, UK, August 23–28, 2020, Proceedings, Part XII 16*, pp. 258–274. Springer, 2020.
- Team, Q. Qwen2.5: A party of foundation models, September 2024. URL <https://qwenlm.github.io/blog/qwen2.5/>.
- Valle, R., Buenaposada, J. M., and Baumela, L. Multi-task head pose estimation in-the-wild. *IEEE Transactions on Pattern Analysis and Machine Intelligence*, pp. 2874–2881, Aug 2021. doi: 10.1109/tpami.2020.3046323. URL <http://dx.doi.org/10.1109/tpami.2020.3046323>.
- Wang, J., Yuan, L., Zhang, Y., and Sun, H. Tarsier: Recipes for training and evaluating large video description models. *arXiv preprint arXiv:2407.00634*, 2024a.
- Wang, P., Bai, S., Tan, S., Wang, S., Fan, Z., Bai, J., Chen, K., Liu, X., Wang, J., Ge, W., et al. Qwen2-vl: Enhancing vision-language model’s perception of the world at any resolution. *arXiv preprint arXiv:2409.12191*, 2024b.
- Wang, X., Zhang, X., Luo, Z., Sun, Q., Cui, Y., Wang, J., Zhang, F., Wang, Y., Li, Z., Yu, Q., et al. Emu3: Next-token prediction is all you need. *arXiv preprint arXiv:2409.18869*, 2024c.
- Wang, Y., Sun, Y., Huang, Y., Liu, Z., Gao, S., Zhang, W., Ge, W., and Zhang, W. Ferv39k: A large-scale multi-scene dataset for facial expression recognition in videos. In *Proceedings of the IEEE/CVF conference on computer vision and pattern recognition*, pp. 20922–20931, 2022.
- Wang, Y., Xu, B., Yue, Z., Xiao, Z., Wang, Z., Zhang, L., Yang, D., Wang, W., and Jin, Q. Timezero: Temporal video grounding with reasoning-guided lvlm. *arXiv e-prints*, pp. arXiv–2503, 2025.
- Wishart, D. S., Guo, A., Oler, E., Wang, F., Anjum, A., Peters, H., Dizon, R., Sayeeda, Z., Tian, S., Lee, B. L., et al. Hmdb 5.0: the human metabolome database for 2022. *Nucleic acids research*, 50(D1):D622–D631, 2022.
- Wolf, L., Hassner, T., and Maoz, I. Face recognition in unconstrained videos with matched background similarity. In *The 24th IEEE Conference on Computer Vision and Pattern Recognition, CVPR 2011, Colorado Springs, CO, USA, 20-25 June 2011*, pp. 529–534. IEEE Computer Society, 2011a. doi: 10.1109/CVPR.2011.5995566. URL <https://doi.org/10.1109/CVPR.2011.5995566>.
- Wolf, L., Hassner, T., and Maoz, I. Face recognition in unconstrained videos with matched background similarity. In *CVPR 2011*, pp. 529–534. IEEE, 2011b.
- Xu, L., Zhao, Y., Zhou, D., Lin, Z., Ng, S. K., and Feng, J. Pllava: Parameter-free llava extension from images to videos for video dense captioning. *arXiv preprint arXiv:2404.16994*, 2024.
- Yang, A., Yang, B., Hui, B., Zheng, B., Yu, B., Zhou, C., Li, C., Li, C., Liu, D., Huang, F., Dong, G., Wei, H., Lin, H., Tang, J., Wang, J., Yang, J., Tu, J., Zhang, J., Ma, J., Xu, J., Zhou, J., Bai, J., He, J., Lin, J., Dang, K., Lu, K., Chen, K., Yang, K., Li, M., Xue, M., Ni, N., Zhang, P., Wang, P., Peng, R., Men, R., Gao, R., Lin, R., Wang, S., Bai, S., Tan, S., Zhu, T., Li, T., Liu, T., Ge, W., Deng, X., Zhou, X., Ren, X., Zhang, X., Wei, X., Ren, X., Fan, Y., Yao, Y., Zhang, Y., Wan, Y., Chu, Y., Liu, Y., Cui, Z., Zhang, Z., and Fan, Z. Qwen2 technical report. *arXiv preprint arXiv:2407.10671*, 2024.
- Yang, A., Li, A., Yang, B., Zhang, B., Hui, B., Zheng, B., Yu, B., Gao, C., Huang, C., Lv, C., et al. Qwen3 technical report. *arXiv preprint arXiv:2505.09388*, 2025a.
- Yang, Q., Bai, D., Peng, Y.-X., and Wei, X. Omni-emotion: Extending video mllm with detailed face and audio modeling for multimodal emotion analysis. *arXiv preprint arXiv:2501.09502*, 2025b.
- Yang, Y., He, X., Pan, H., Jiang, X., Deng, Y., Yang, X., Lu, H., Yin, D., Rao, F., Zhu, M., et al. R1-onevision: Advancing generalized multimodal reasoning through cross-modal formalization. *arXiv preprint arXiv:2503.10615*, 2025c.
- Yu, Q., Zhang, Z., Zhu, R., Yuan, Y., Zuo, X., Yue, Y., Dai, W., Fan, T., Liu, G., Liu, L., et al. Dapo: An open-source llm reinforcement learning system at scale. *arXiv preprint arXiv:2503.14476*, 2025.
- Zhang, H., Li, X., and Bing, L. Video-llama: An instruction-tuned audio-visual language model for video understanding. *arXiv preprint arXiv:2306.02858*, 2023a.
- Zhang, J., Huang, J., Yao, H., Liu, S., Zhang, X., Lu, S., and Tao, D. R1-vl: Learning to reason with multimodal large language models via step-wise group relative policy optimization. *arXiv preprint arXiv:2503.12937*, 2025.
- Zhang, K., Zhang, Z., Li, Z., and Qiao, Y. Joint face detection and alignment using multi-task cascaded convolutional networks. *IEEE Signal Processing Letters*, pp. 1499–1503, Oct 2016. doi: 10.1109/lsp.2016.2603342. URL <http://dx.doi.org/10.1109/lsp.2016.2603342>.
- Zhang, X., Li, M., Lin, S., Xu, H., and Xiao, G. Transformer-based multimodal emotional perception for dynamic facial expression recognition in the wild. *IEEE Transactions on Circuits and Systems for Video Technology*, 34(5):3192–3203, 2023b.

- Zhang, Y., Li, B., Liu, H., Lee, Y., Gui, L., Fu, D., Feng, J., Liu, Z., and Li, C. Llava-next: A strong zero-shot video understanding model. 2024.
- Zhao, J., Sun, B., Chen, X., and Wei, X. Facial dynamics in video: Instruction tuning for improved facial expression perception and contextual awareness. *arXiv preprint arXiv:2501.07978*, 2025a.
- Zhao, J., Wei, X., and Bo, L. R1-omni: Explainable omni-multimodal emotion recognition with reinforcement learning. *arXiv preprint arXiv:2503.05379*, 2025b.
- Zhao, J., Yang, Q., Peng, Y., Bai, D., Yao, S., Sun, B., Chen, X., Fu, S., Wei, X., Bo, L., et al. Humanomni: A large vision-speech language model for human-centric video understanding. *arXiv preprint arXiv:2501.15111*, 2025c.
- Zhao, Z. and Patras, I. Prompting visual-language models for dynamic facial expression recognition. *arXiv preprint arXiv:2308.13382*, 2023.
- Zheng, Y., Yang, H., Zhang, T., Bao, J., Chen, D., Huang, Y., Yuan, L., Chen, D., Zeng, M., and Wen, F. General facial representation learning in a visual-linguistic manner. In *2022 IEEE/CVF Conference on Computer Vision and Pattern Recognition (CVPR)*, Jun 2022. doi: 10.1109/cvpr52688.2022.01814. URL <http://dx.doi.org/10.1109/cvpr52688.2022.01814>.
- Zhu, B., Lin, B., Ning, M., Yan, Y., Cui, J., Wang, H., Pang, Y., Jiang, W., Zhang, J., Li, Z., et al. Language-bind: Extending video-language pretraining to n-modality by language-based semantic alignment. *arXiv preprint arXiv:2310.01852*, 2023a.
- Zhu, D., Chen, J., Shen, X., Li, X., and Elhoseiny, M. Minigpt-4: Enhancing vision-language understanding with advanced large language models. *arXiv preprint arXiv:2304.10592*, 2023b.
- Zhu, H., Wu, W., Zhu, W., Jiang, L., Tang, S., Zhang, L., Liu, Z., and Loy, C. C. Celebv-hq: A large-scale video facial attributes dataset. In *European conference on computer vision*, pp. 650–667. Springer, 2022.

## A. Related Works

The rapid advancement of multimodal large language models (MLLMs) has spurred the emergence of Video-MLLMs. To mitigate the dramatic increase in visual token count caused by the temporal dimension, existing approaches typically either insert projectors such as MLPs and Q-Formers (Li et al., 2023a) after the visual encoder (Maaz et al., 2023; Xu et al., 2024; Ma et al., 2023; Li et al., 2023b; Liu et al., 2024) or train a dedicated video encoder from scratch (Maaz et al., 2023; Luo et al., 2023; Ren et al., 2024; Wang et al., 2024c). However, these strategies often sacrifice fine-grained features particularly in domains with rich and intricate details such as human faces. While significant progress has been achieved in fine-grained facial understanding for static images (Narayan et al., 2024; Sun et al., 2024b; Qin et al., 2024; 2023), extending such capabilities to videos remains underexplored, with few high-performance frameworks designed specifically for fine-grained video face analysis. This gap represents one of the key challenges that our proposed FaVChat addresses. Unlike static face images, facial videos contain additional temporal cues, such as inter-frame facial motion and emotional dynamics, necessitating models that go beyond superficial appearance and capture deeper semantic content. Reinforcement learning (RL) (Shao et al., 2024) offers a promising avenue to enhance such understanding; however, current label-free preference-based RL methods struggle to supervise fine-grained descriptions (Wang et al., 2025; Zhao et al., 2025b; Feng et al., 2025), while obtaining fine-grained annotations is prohibitively labor-intensive, which is a dual challenge that FaVChat seeks to overcome. Below is a more comprehensive discussion of related work.

### A.1. Video Multimodal Large Language Models

With the rapid advancement of Multimodal Large Language Models (MLLMs), the research community has increasingly shifted its focus towards video. Unlike images, videos introduce an additional temporal dimension, which leads to a multiplicative increase in the number of visual tokens that MLLMs need to process. This complexity has posed significant challenges to the development of Video-MLLMs. On one hand, similar to MLLMs, the projectors of Video-MLLMs are primarily categorized into two types: MLPs and Q-Formers (Li et al., 2023a). MLP-based frameworks directly transform the output of the visual encoder into embeddings. For instance, Video-ChatGPT (Maaz et al., 2023) aligns video features with the LLM through linear layers, while PLLaVA (Xu et al., 2024) employs pooling to mitigate domain differences between images and videos. However, the inherent structure of MLPs limits their capability in handling multi-frame videos. In contrast, the output of Q-Formers is independent of the length of the input video and is instead determined by the number of learnable queries. For example, Vista-LLaMA (Ma et al., 2023) integrates a recursive approach into the application of Q-Former, aiming to address the limited frame differentiation problem of Q-Former. VideoChat (Li et al., 2023b) utilizes additional learnable queries to align video embeddings. ST-LLM (Liu et al., 2024) directly applies a pre-trained Q-Former to video frames, resulting in more compact representations.

On the other hand, since videos can be decomposed into sequences of images, the majority of current research still employs image encoders to extract features from video frames as video representations. For instance, VideoChat (Li et al., 2023b), Video-ChatGPT (Maaz et al., 2023), Valley (Luo et al., 2023), and Chat-UniVi (Jin et al., 2024) utilize CLIP ViT (Long et al., 2015) to process videos, while LLaMA-VID (Li et al., 2024c), TimeChat (Ren et al., 2024), and Emu3 (Wang et al., 2024c) opt for Eva-clip ViT (Sun et al., 2023b) as their visual encoder. However, treating videos merely as sequences of images overlooks the temporal characteristics of videos. Consequently, subsequent researchers advocate employing pre-trained video encoders to capture temporal features. For example, VideoChat2 (Li et al., 2024b) adopts the pre-trained video foundation model UMT-L (Li et al., 2023c) to capture video features, and Video-LLaVA (Lin et al., 2023) leverages the visual encoder of languageBind (Zhu et al., 2023a) to process video inputs. Nevertheless, while these methods aim to increase the length of comprehensible videos, they neglect the importance of fine-grained information, resulting in the loss of fine-grained features.

### A.2. Fine-grained Facial Understanding

The task of fine-grained face understanding aims to capture, parse, and comprehend the detailed features of the human face, and to apply the obtained results to various practical applications. Research in this area based on still images has achieved remarkable performance. Tasks such as face parsing (Kuprashevich & Tolstykh, 2023; Te et al., 2020), facial attribute recognition (Shu et al., 2021; Zheng et al., 2022), age/gender estimation (Cao et al., 2020; Kuprashevich & Tolstykh, 2023), head pose estimation (Cobo et al., 2024; Valle et al., 2021), and facial expression recognition (Chang et al., 2018; Li & Deng, 2020) have been extensively studied by the academic community. In addition, subsequent researchers have attempted to build multi-task models to handle multiple tasks using a single general model (Zhang et al., 2016; Ranjan

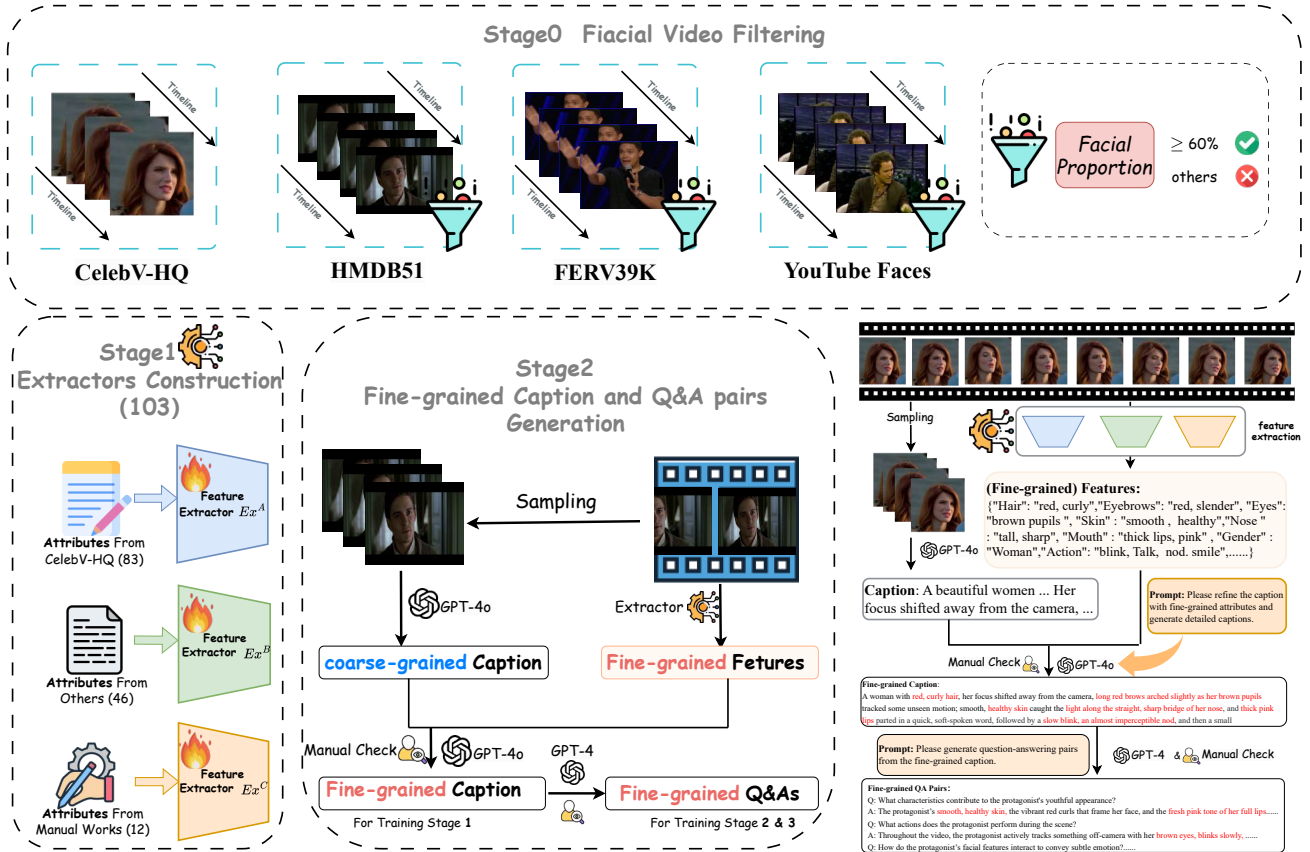


Figure 9. Training Data Creation Process.

et al., 2019; 2016). However, common multi-task models are only capable of performing tasks that are highly correlated. This dilemma has been alleviated with the development of transformers. Face perception models based on transformers, such as FaceXFormer (Narayan et al., 2024), Q-Face (Sun et al., 2024b), Faceptor (Qin et al., 2024), and SwinFace (Qin et al., 2023), have brought convenience to the research of fine-grained face understanding. Notably, FaceXFormer (Narayan et al., 2024) introduced FaceX, an efficient parameterized decoder that provides a universal facial feature representation for multi-tasking. Our proposed FaVChat incorporates FaceXFormer (Narayan et al., 2024) as an additional visual encoder, focusing on extracting visual facial features. However, despite the significant progress made in the image domain, there is still a lack of research on high-performance fine-grained video face understanding frameworks when extending the task of fine-grained face understanding to the video domain. This is the focus of the current paper.

### A.3. Reinforcement Learning for Video-MLLMs

With the remarkable success of multimodal large language models (MLLMs) (Deng et al., 2025a;b; Liu et al., 2025b; Zhang et al., 2025), reinforcement learning has been increasingly extended to video understanding. Early approaches, such as TimeZero (Wang et al., 2025) and R1-Omni (Zhao et al., 2025b), applied GRPO (Shao et al., 2024) to video tasks involving temporal distribution modeling and sentiment analysis. Video-R1 (Feng et al., 2025) enhanced spatial reasoning in videos by integrating spatiotemporal sequential structure into GRPO. Building upon this, STAR-R1 (Qi et al.) introduced a tailored spatiotemporal reward mechanism to further improve the model’s reasoning capabilities in dynamic, long-duration scenarios. In this work, we propose DE-GRPO, a novel reinforcement learning framework specifically designed for data-efficient training with limited high-quality samples. Experimental results show that our method achieves substantial performance gains across a range of face-centric video understanding tasks.

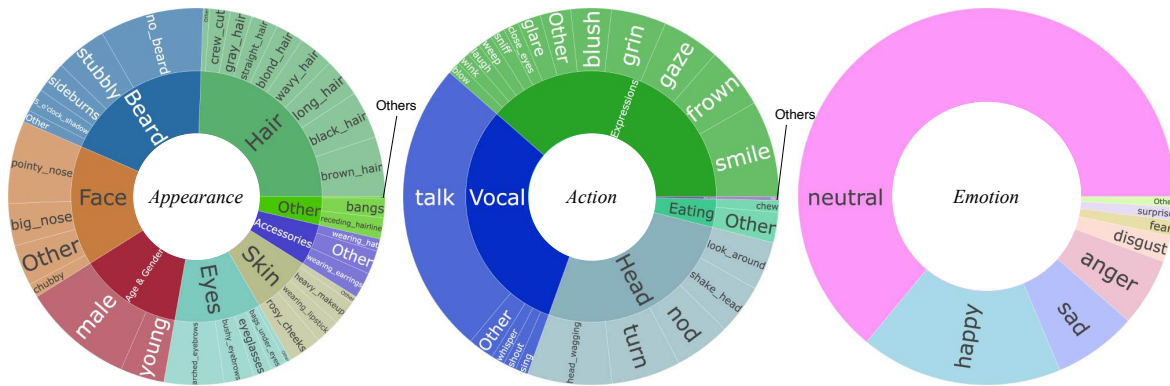


Figure 10. Distribution of the FaVChat dataset. For clarity, low-frequency attributes are grouped into an "Other" category.

Table 5. Attribute statistics results of FaVChat dataset. The first row denotes the attribute names, and the second line denotes the occurrence counts of corresponding attributes in the dataset.

Appearance									
blurry	male	young	chubby	pale_skin	rosy_cheeks	oval_face	receding_hairline	bald	bangs
610	38434	15252	4880	2440	11591	3660	7321	1830	6711
black_hair	blond_hair	gray_hair	brown_hair	straight_hair	wavy_hair	long_hair	arched_eyebrows	bushy_eyebrows	bags_under_eyes
16472	9761	7626	20742	9151	12201	13422	20742	10371	5491
eyeglasses	sunglasses	narrow_eyes	big_nose	pointy_nose	high_cheekbones	big_lips	double_chin	no_beard	5_o'clock_shadow
6467	1834	1220	14621	28674	3672	2928	2671	35994	7981
goatee	sideburns	mustache	heavy_makeup	wearing_earrings	wearing_hat	wearing_lipstick	wearing_necklace	wearing_necktie	wearing_mask
976	10981	2478	8541	8976	4271	8663	3663	3512	1021
facial_tattoos	facial_hair	clean_shaven	stubbly	shaved_head	crew_cut	mullet	bald_spot		
244	126	421	17784	276	7123	62	42		
Action									
blow	chew	close_eyes	cough	cry	drink	eat	frown	gaze	glare
1961	1891	2441	51	692	1161	1432	9761	9151	3678
head_wagging	kiss	laugh	listen_to_music	look_around	make_a_face	nod	play_instrument	read	shake_head
13421	918	2189	1513	7688	107	8907	102	811	7931
shout	sign	sing	sleep	smile	smoke	sneeze	sneer	sniff	talk
2032	1712	2001	599	15241	1271	22	1621	2318	46775
turn	weep	whisper	wink	yawn	blush	grin	grimace	scrunch	squint
10981	2271	2121	2098	92	6421	8724	102	812	92
stare	smirk	sigh	pout	wince					
651	61	118	141	271					
Emotion									
happy	sad	surprise	neutral	anger	contempt	disgust	fear	Shame	Confusion
10798	4472	726	39869	3629	469	1403	836	31	36

## B. Dataset

In this section, we provide a detailed description of the dataset and its construction pipeline. To the best of our knowledge, our dataset is the only face video dataset that includes question-answer annotations and features the largest number of attribute categories. Specifically, it comprises 61,007 high-resolution videos, each annotated with 2 to 4 question-answer pairs and a caption of over 100 tokens. The dataset encompasses 103 attributes, more than any existing face video dataset. Fig. 5 compares our dataset with current popular "face-centric" datasets. Additionally, the distribution of attribute counts is shown in Figure 10, and the attribute statistics are summarized in Table 5. The construction pipeline consists of three stages: face video filtering, extractor construction, and fine-grained caption and question-answer pair generation. A concrete example is provided in the bottom-right corner of Fig. 9. Detailed descriptions are given in the following subsections.

### B.1. Filtering Facial Videos from Existing datasets

Our video raw data consists of four parts: CelebV-HQ (Zhu et al., 2022), HMDB51 (Kuehne et al., 2011), FERV39K (Wang et al., 2022) and YouTube Faces (Wolf et al., 2011a). Specifically, given the detailed video attributes of CelebV-HQ, we have incorporated all 35,666 video from CelebV-HQ. For other videos, we first conducted face detection utilizing AntelopeV2 (Ren et al., 2023). If the minimum proportion of human faces in the video exceeded 60%, the video was considered to meet

**Algorithm 1** Weight Adapter Algorithm

---

```

1: Input:  $\mathbf{V} \in \{\mathbf{V}_g, \mathbf{V}_f\} \in \mathbb{R}^{L \times d}$ ,  $\mathbf{T} \in \mathbb{R}^{L \times d}$  Visual and text tokens
2: Initialize:  $W_Q^v \in \mathbb{R}^{d \times d}$ ,  $W_K^t \in \mathbb{R}^{d \times d}$ ,  $W_V^t \in \mathbb{R}^{d \times d}$  Learnable weights
3:  $Q_t \leftarrow TW_Q^t$ ,  $K_v \leftarrow VW_K^v$ ,  $V_v \leftarrow VW_V^v$  Projection to Q, K, V spaces
4:  $A \leftarrow \text{softmax}\left(\frac{Q_t K_v^\top}{\sqrt{d}}\right)$  Attention weights
5:  $H \leftarrow AV_v$  Weighted aggregation
6:  $\tilde{V} \leftarrow \text{LayerNorm}(V + H)$  Residual connection and normalization
7:  $v_{\text{global}} \leftarrow \frac{1}{L} \sum_{i=1}^L \tilde{V}_i$  Global pooling
8:  $h_1 \leftarrow \text{GELU}(W_1 v_{\text{global}} + b_1)$ ,  $h_2 \leftarrow \text{GELU}(W_2 h_1 + b_2)$  MLP layers
9:  $\text{output} \leftarrow w^\top h_2 + b$  Final output
10: Return output

```

---

**Algorithm 2** DE-GRPO

---

```

1: Initialize  $D$ ,  $\theta$ , and other hyperparameters
2: for  $i = 0$  to total_items do
3:   Sample batch  $B$  from  $D$ 
4:   for data  $\in B$  do
5:     Compute  $U^{(i)}$  (Refer to Equation 10)
6:     Update  $s^{(i+1)}$  (Refer to Equation 11)
7:     if  $s^{(i+1)} < \tau_{\text{remove}}$  then
8:       Remove  $i$  from  $D_t$ 
9:     continue
10:  end for
11:  Set  $\delta(i)$  (Refer to Equation 12)
12:  Compute  $\bar{A}^{(i)}$  (Refer to Equation 13)
13: end for
14: Optimize  $L_{\text{SF-RDF}}$  (Refer to Equation 16)
15: end for

```

---

the face video standard. Subsequently, based on the average length of videos in CelebV-HQ, we used the OpenCV package to trim the videos, ultimately obtaining an additional 25,341 video clips, each ranging in length from 36 to 600 frames.

**B.2. Fine-grained Feature Extractors Construction**

To ensure the extraction of a rich set of fine-grained features from each video, we developed a multi-classifier feature extractor. Initially, we sample 1,000 data points from CelebV-HQ and another 1,000 from the combined HMDB51, FERV39K, and YouTube Faces datasets. These samples were used to train two multi-classifiers:  $Ex^A$ , capable of extracting 83 facial features, and  $Ex^B$ , which extracts 42 facial features. However, these features still lacked descriptions of subtle facial micro-expressions (e.g., eyebrow raises, frowns, pouts).

To address this, we additionally sample 452 videos from CelebV-HQ, specifically chosen for their pronounced facial actions. These videos underwent meticulous manual annotation for micro-expression features, which then served as training data for a third multi-classifier,  $Ex^C$ . This classifier was designed to extract 12 distinct micro-expression features. Our comprehensive feature extractor, as illustrated in step 1 of Fig. 9, integrates these three classifiers. After eliminating redundant features, this combined extractor captures a total of 103 facial features. To our knowledge, this represents the largest number of features extracted in the field of facial video analysis, thereby guaranteeing the availability of sufficiently rich, fine-grained labels for our training data.

**B.3. Generating Text for Each Video**

We’ve outlined a detailed process for generating textual descriptions from original videos, as depicted in step 2 of Fig. 9. The video textual generation process is further divided into four sub-steps:

- **Frame Sequence Generation.** The raw video frames are down sample by 16 to obtain a shorter frame sequence.
- **Fine-grained Description Generation.** We feed the frame sequence from the preceding step to the trained feature extractors. And the output is subsequently converted into a fine-grained feature dictionary via rule-based textual mapping.
- **Summary Generation.** we input the frame sequence obtained in the first sub-step and the fine-grained feature dictionary derived in the second sub-step into GPT-4o with an engineered prompt to generate fine-grained summary texts.
- **QA Pair Generation.** we employ GPT-4 to generate 4 question-answer (QA) pairs for each summary obtained in the third sub-step.

Note that in sub-steps 3 and 4, we implement manual quality control through sampling during the generation process.

Additionally, we conduct multiple rounds of random sampling on the generated text, followed by rigorous human evaluation to ensure that the textual quality meet the stringent requirements for model training.

### C. Implementation Details

We use Qwen2.5-7B (Yang et al., 2024; Team, 2024) as the backbone LLM, with UMT-L (Li et al., 2023b; 2024b) as the general visual encoder and the FaceXFormer feature extractor (Narayan et al., 2024) as the facial encoder. A lightweight Q-Former (Li et al., 2023a) together with two linear layers serves as the projection module. All experiments are conducted on 8 NVIDIA A100 GPUs. In the three-stage fine-tuning pipeline, we use a learning rate of  $2 \times 10^{-4}$  with a batch size of 16 in the first stage, keep the same learning rate but reduce the batch size to 8 in the second stage, and adopt a learning rate of  $2 \times 10^{-5}$  with a batch size of 8 in the final stage. During reinforcement learning, we further lower the learning rate to  $2 \times 10^{-6}$ , use a batch size of 8, and set the weight decay to 0.8.

### D. RL Supplement

In Sec. 2.2 of the main text, the data recurrent mechanism in DE-GRPO, which is grounded in data efficiency, is introduced, and the reinforcement learning advantage function  $\bar{A}^{(i)}$  derived from this mechanism is described. We now provide a complete specification of the DE-GRPO procedure.

After obtaining the advantage function based on the data recurrent mechanism, we substitute it into the GRPO formulation. First, we define the following:

$$\rho_w^{(i)} = \frac{\pi_\theta(y_w^{(i)} | x^{(i)})}{\pi_{\text{old}}(y_w^{(i)} | x^{(i)})}, \quad \rho_l^{(i)} = \frac{\pi_\theta(y_l^{(i)} | x^{(i)})}{\pi_{\text{old}}(y_l^{(i)} | x^{(i)})}, \quad (14)$$

$$\Delta^{(i)} = \rho_w^{(i)} - \rho_l^{(i)}, \quad (15)$$

where  $i$  denotes the iteration index of the data recurrent mechanism, and the overall objective function of DE-GRPO is as follows:

$$\mathcal{J}_{\text{DE-GRPO}} = \mathbb{E}_{\mathcal{B}_t} \left[ \min \left( \log \sigma(\Delta^{(i)}) \cdot \bar{A}^{(i)}, \log \sigma(\text{clip}(\Delta^{(i)}, 1 - \epsilon, 1 + \epsilon)) \cdot \bar{A}^{(i)} \right) + \beta \text{KL}[\pi_\theta \| \pi_{\text{ref}}] \right] \quad (16)$$

We present the complete DE-GRPO procedure in Algorithm 2 and summarize the associated parameters in Table 6.

**Rationale for the Decay Factor Design.** In Equation 12, the decay factor  $\delta^{(i)}$  is designed to govern the dynamic lifecycle of training samples and prevent overfitting. Intuitively, one might expect high-utility samples (where  $s^{(i)} > \tau_{\text{keep}}$ ) to be retained with a high weight. However, if we assign a factor  $\geq 1$  to these samples, their accumulated score  $s^{(i)}$  would monotonically increase, causing them to permanently dominate the training batch. This would lead to two issues: (1) the model would overfit to these specific samples, and (2) new, potentially informative samples would be blocked from entering the active training set. Therefore, we set  $\delta < 1$  (e.g., 0.5) specifically when  $s^{(i)}$  exceeds the upper threshold  $\tau_{\text{keep}}$ . This mechanism acts as a ‘‘cooling-down’’ strategy: once a sample has been identified as high-utility and utilized for training, we explicitly reduce its priority to reflect the diminishing marginal returns of repeated learning. Conversely, for samples in the intermediate range ( $\tau_{\text{remove}} \leq s^{(i)} \leq \tau_{\text{keep}}$ ), we set  $\delta^{(i)} = 1$  to allow them to accumulate utility scores based on their merit until they either prove useful enough to trigger the training threshold or fade out to be discarded. This design ensures a continuous flow of data where samples are discovered, exploited, and eventually deprecated.

**Clarification on Sample-Level Advantage.** A critical distinction between standard GRPO (Shao et al., 2024) and our proposed DE-GRPO lies in the granularity of the advantage function. In standard GRPO, the advantage is computed per response to estimate the relative quality of each generated output against the group baseline. In contrast, DE-GRPO aims

Table 6. Statistical results of hyperparameters appearing in DE-GRPO

Symbol	Meaning	Value in FaVChat
$\lambda$	Recurrent smoothing	0.8
$\tau_{\text{remove}}$	Remove threshold	0.20
$\tau_{\text{keep}}$	Keep threshold	0.80
$\delta$	Reward decay factor	0.50
$\epsilon$	PPO clip	0.20
$\beta$	KL coefficient	0.01

to optimize data efficiency by prioritizing high-utility training samples. Consequently, the advantage  $\bar{A}^{(i)}$  in Equation 13 is computed as an average scalar shared across all response pairs  $\mathcal{P}$  derived from the same input video  $x^{(i)}$ . Here,  $\bar{A}^{(i)}$  functions as a *sample-level importance weight* rather than a *response-level alignment signal*. It scales the gradient updates based on the sample’s current utility: inputs that yield highly separable rewards (indicating rich learning signals) are assigned larger advantage values, thereby amplifying their contribution to the policy update. This design ensures that the model focuses its capacity on learning from the most informative video samples in each iteration.

## E. Adapter Supplement

This section serves as a supplement to Section Sec. 2.1 of the main text where we formally describe FaVChat’s high-level prompt-query learning. Specifically, two independent learnable weight adapters integrate visual features and prompt-query textual features, producing corresponding learnable scalars. We provide the associated pseudocode implementation in Algorithm 1.

The two independent weight adapters employ the same training strategy and produce separate scalar outputs, which are then normalized using softmax to generate complementary weighting coefficients.

## F. The complete results of Textual Facial Analysis

In this section, we present all experimental results on the DFEC dataset, summarized in Tab. 7. The proposed FaVChat model achieves superior performance across all existing VLLMs.

Table 7. Performance comparison on the DFEC (Zhao et al., 2025a) dataset for textual emotion analysis. The \* columns show VideoChatGPT Scores (0–10) evaluated on our internally curated test dataset. ♣ denotes a model trained to process both visual and speech modalities. "-Face" denotes the variant fine-tuned on our FaVChat-170K dataset.

Method	LLM	VideoChatGPT Scores					N-gram Based		Event Based
		Size	Test(2000)*	Correctness	Detail	Context	Temporal	CIDeR	Rouge-L
<i>General VLLM</i>									
VideoLLaMA (Zhang et al., 2023a)	7B	6.12	3.60	3.67	3.84	3.50	0.189	0.196	0.303
VideoChat (Li et al., 2023b)	7B	5.92	3.47	3.52	3.92	3.38	0.251	0.192	0.344
VideoChat2 (Li et al., 2024b)	7B	6.47	3.70	3.56	4.16	3.52	0.202	0.229	0.311
Chat-UniVI (Jin et al., 2024)	7B	6.76	3.64	3.63	4.21	3.61	0.189	0.231	0.396
LLaVA-Next-Video (Zhang et al., 2024)	7B	7.14	4.19	4.07	4.39	4.04	0.250	0.249	0.395
ShareGPT4Video (Chen et al., 2024b)	7B	7.33	4.24	4.13	4.35	4.09	0.192	0.205	0.394
LLaMA-VID (Li et al., 2024c)	7B	6.98	3.95	4.01	4.22	3.71	0.195	0.231	0.339
VideoLLaMA2 (Cheng et al., 2024)	7B	7.41	4.17	4.02	4.47	3.93	0.253	0.266	0.344
PLLaVA (Xu et al., 2024)	7B	7.47	4.21	4.15	4.37	4.08	0.268	0.250	0.393
ST-LLM (Liu et al., 2024)	7B	6.79	4.00	3.98	4.31	3.94	0.213	0.238	0.321
Tarsier (Wang et al., 2024a)	7B	6.42	3.59	3.50	4.07	3.41	0.143	0.185	0.415
LLaVA-OneVision (Li et al., 2024a)	7B	6.72	3.68	3.47	4.10	3.42	0.115	0.165	0.379
Qwen2.5-VL-7B (Bai et al., 2025b)	7B	7.84	4.49	4.36	4.43	4.21	0.261	0.254	0.417
Qwen2.5-VL-72B (Bai et al., 2025b)	72B	8.47	4.61	4.47	4.59	4.78	0.281	0.317	0.453
Qwen2.5-VL-3B (Bai et al., 2025b)	2B	7.01	4.01	3.98	4.37	3.88	0.202	0.221	0.406
Qwen3-VL-8B (Bai et al., 2025a)	8B	7.99	4.49	4.37	4.41	4.33	0.262	0.257	0.421
Qwen3-VL-30B-A3B (Bai et al., 2025a)	30B	8.44	4.63	4.51	4.57	4.81	0.304	0.331	0.461
Claude4-Sonnet (Anthropic, 2025)	-	7.84	4.55	4.64	4.77	4.84	0.312	0.342	0.472
GPT-4o (OpenAI, 2024)	-	7.67	4.22	3.97	4.48	3.90	0.264	0.213	0.432
<i>Human-Centric VLLM</i>									
Face-MLLM (Sun et al., 2024a)	7B	6.62	3.31	3.54	3.79	2.67	0.204	0.197	0.304
FaceTrack-MM (Zhao et al., 2025a)	7B	7.47	4.42	4.30	4.60	4.26	0.418	0.473	0.483
Qwen2.5-VL-7B-Face (Bai et al., 2025b)	7B	8.64	4.51	4.41	4.45	4.22	0.274	0.261	0.463
Qwen3-VL-8B-Face (Bai et al., 2025a)	8B	8.87	4.58	4.46	4.47	4.51	0.297	0.312	0.429
Emotion-LLaMA* (Cheng et al., 2025)	7B	7.42	4.17	4.33	4.54	4.19	0.294	0.413	0.372
HumanOmni* (Zhao et al., 2025c)	7B	7.51	4.58	4.41	4.70	4.41	0.412	0.468	<b>0.523</b>
Omni-Emotion* (Yang et al., 2025b)	7B	7.53	4.57	4.38	4.73	4.24	0.407	0.461	0.504
<b>FaVChat</b> <sub>Qwen2.5</sub>	7B	8.89	4.84	4.79	4.69	4.78	0.443	0.454	0.487
<b>FaVChat</b> <sub>Qwen3</sub>	8B	<b>9.01</b>	<b>4.87</b>	<b>4.82</b>	<b>4.74</b>	<b>4.81</b>	<b>0.447</b>	<b>0.469</b>	<b>0.523</b>

## G. Ablation: Hierarchical Prompt-Query Learning

As discussed in Sec. 2.3, the distinct training stages of FaVChat correspond to feature learning at progressively higher levels of abstraction. To validate the effectiveness of our hierarchical prompt-guided feature learning approach, we partitioned the internal dataset (introduced in Sec. 3.2) into three test sets reflecting increasing feature levels. Specifically, the low-level test set comprises cases involving only basic facial textures (e.g., skin, hair). The mid-level test set extends this by incorporating cases covering fine-grained facial regions (e.g., eyes, nose, mouth). The high-level test set retains

Table 8. Ablation study results on hierarchical prompt-query learning in FaVChat

model	Test <sub>low</sub>	Test <sub>mid</sub>	Test(2,000) <sub>high</sub>
FaVChat <sub>Stage1</sub>	8.13	6.14	5.18
FaVChat <sub>Stage2</sub>	8.67	8.23(2.09 ↑)	6.37
FaVChat <sub>Stage3</sub>	8.91	8.44	8.31(1.94 ↑)
FaVChat	-	-	8.89

the complete in-house test set of 2,000 samples. We then evaluate FaVChat at each training stage across all three test sets to assess the developmental trajectory of feature representation learning. The quantitative results are summarized in Table 8. Experimental results demonstrate that the performance on the internal dataset progressively improves as training proceeds through successive stages. Specifically, FaVChat in Stage 1 excels only on the low-level test set, while Stage 2 exhibits a significant improvement on the medium-level test set, and Stage 3 achieves notable performance even on the high-level test set. This progression validates the effectiveness of our hierarchical feature learning approach.

## H. Statement on Ethics, Privacy, and Bias

All original facial videos in our proposed FaVChat-170K dataset are sourced from open-source video datasets that have undergone rigorous review and formal ethical risk assessment. Additionally, during the generation of summaries and question-answer pairs, we rigorously monitored and regulated the model’s generation process to mitigate ethical risks—specifically discrimination related to sociodemographic factors, race, or gender—thereby ensuring compliance with established academic ethics standards.

## I. More Zero-shot Generalizations

**Face Recognition.** Face recognition can be viewed as a matching task in which two facial video clips are compared to determine whether they belong to the same individual. The YouTube Faces dataset is well suited for this setting, as it contains multiple videos per person under diverse conditions. Using this dataset, we construct a test set of 3,190 video segments from YouTube Faces (Wolf et al., 2011a) that are excluded from training. Each segment contains 36 frames and covers a total of 1,595 unique identities. We evaluate this test set on several models, including GPT-4o (Hurst et al., 2024), Claude-4-Sonnet (Anthropic, 2025), VideoChat (Li et al., 2023b), VideoChat2 (Li et al., 2024b), Qwen2.5-VL (2B, 7B, 72B) (Wang et al., 2024b), and VideoLLaMA2 (Cheng et al., 2024), using accuracy as the metric.

Table 9. Comparisons of different methods on the facial recognition task. “w. FaVChat” denotes that fine-grained facial features extracted by FaVChat are provided as additional inputs to MLLMs, enhancing their decision-making process.

Methods	Size	Acc	Acc <sub>w. FaVChat</sub>
GPT-4o (OpenAI, 2024)	-	71.29	93.61
Claude4-Sonnet (Anthropic, 2025)	-	73.41	<b>96.14</b>
VideoChat (Li et al., 2023b)	7B	54.74	73.61
VideoChat2 (Li et al., 2024b)	7B	57.30	81.32
VideoLLaMa2 (Cheng et al., 2024)	7B	51.03	75.05
Qwen2.5-VL-7B-Face (Bai et al., 2025b)	7B	64.28	85.58
Qwen2.5-VL-72B (Bai et al., 2025b)	72B	66.84	85.87
<b>FaVChat</b>	7B	<b>88.38</b>	-

As shown in Table 9, FaVChat achieves state of the art performance on the facial recognition task. Moreover, when fine grained facial features extracted by FaVChat are used as inputs to other models, all of them exhibit clear performance gains. This further highlights FaVChat’s strong ability to capture fine grained facial information, which is crucial for accurate face recognition.

**Explainable Multimodal Emotion Reasoning.** The creation of the EMER dataset (Lian et al., 2023) highlights an important insight for the community: when additional multimodal emotional cues, such as subtle facial movements, contextual video information, and emotional categories, are incorporated, interpretable emotional reasoning becomes more critical than mere emotion recognition. To evaluate this aspect, we assess FaVChat on the Explainable Multimodal Emotional Reasoning (EMER) task. Following prior works, we employ GPT-4o for evaluation, measuring performance using two key metrics: (1) overlap of relevant cues and (2) overlap of final emotional states. The results, shown in Table 10, demonstrate that FaVChat consistently outperforms existing models on both metrics, validating its ability to leverage fine-grained multimodal cues for enhanced emotional reasoning.


Table 10. Comparison of explainable multimodal emotion reasoning performance on the EMER dataset (Lian et al., 2023).

Models	Clue Overlap	Label Overlap
Ground Truth	10.0	10.0
VideoChat-Text (Li et al., 2023b)	6.32	3.97
Video-LLaMA (Zhang et al., 2023a)	6.51	4.72
Video-ChatGPT (Maaz et al., 2023)	6.98	5.79
PandaGPT (Su et al., 2023)	7.15	5.49
VideoChat-Embed (Li et al., 2023b)	7.15	5.65
Valley (Luo et al., 2023)	7.31	5.76
<b>FaVChat</b>	<b>8.41</b>	<b>7.01</b>

## J. Clarify of Large Language Models Usage

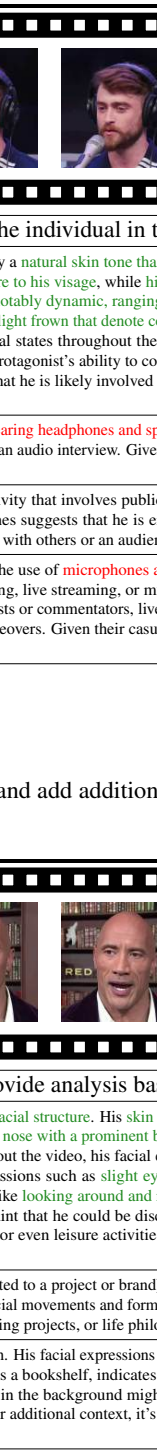
We clarify that the LLMs were used solely for writing assistance and language editing (*e.g.*, enhancing textual clarity and correcting grammatical errors). All outputs presented in this paper have been verified by the authors.

Table 11. We randomly sample multiple qualitative comparison cases (1/4) and add additional color labeling to the content involving fine-grained facial features.



Question	What could be the possible profession or activity of the individual in the video?
FaVChat	The individual in the video presents a detailed facial profile characterized by a <b>natural skin tone</b> that hints at signs of fatigue, such as bags under the eyes, suggesting a demanding lifestyle. His <b>pointy nose</b> adds a unique feature to his visage, while his <b>brown hair and bushy eyebrows</b> frame his face, contributing to a distinctive appearance. The protagonist's expressions are notably dynamic, ranging from a slight raise of the eyebrows and upward curve of the mouth indicating laughter, to a tightening around the eyes and a slight frown that denote contemplation or concern. These microexpressions, combined with the <b>potential changes in pupil size</b> , reflect varying emotional states throughout the video. The <b>gentle smile that forms by the final image</b> suggests a return to a more relaxed or positive state, highlighting the protagonist's ability to convey a spectrum of emotions. This detailed facial description, along with the professional headset and microphone, suggests that he is likely involved in a communication-intensive profession such as broadcasting, podcasting, or live streaming.
Qwen3-VL-8B-Face	The individual is likely engaged in radio broadcasting or podcasting. He is <b>wearing headphones and speaking into a professional microphone</b> , which are typical tools for hosting a radio show, recording a podcast, or participating in an audio interview. Given his setup, he could be a radio host, podcaster, or a guest being interviewed for an audio program.
GPT-4o	Based on this Video, the individual is likely engaged in a profession or activity that involves public speaking or broadcasting, such as a radio host, podcaster, or commentator. The presence of the microphone and headphones suggests that he is either recording audio content, live streaming, or participating in a broadcast where he needs to hear and communicate clearly with others or an audience.
Qwen3-VL-30B-A3B	The individuals in the video appear to be engaged in activities that require the use of <b>microphones and headphones</b> , which are often associated with professions or activities such as podcast recording, voice acting, radio hosting, live streaming, or music production. They may be recording podcast programs, providing audio for animations or audiobooks, serving as radio hosts or commentators, live streaming games or topic discussions on Twitch or YouTube, or participating in music production by providing vocals or voiceovers. Given their casual attire and focused expressions, it is most likely that they are engaged in podcast recording, voice acting, or live streaming.

Table 12. We randomly sample multiple qualitative comparison cases (2/4) and add additional color labeling to the content involving fine-grained facial features.



Question	What might the protagonist be discussing? Please provide analysis basis.
FaVChat	The protagonist in the video is a male with a bald head and a strong, mature facial structure. His skin is smooth with minimal aging signs, and his dark, well-defined pupils convey an intense and focused gaze. He possesses a large nose with a prominent bridge and slightly rounded tip, which, along with his bushy eyebrows, forms a distinctive central feature of his face. Throughout the video, his facial expressions are <b>predominantly neutral</b> , reflecting confidence and composure, yet he occasionally exhibits subtle microexpressions such as <b>slight eyebrow movements</b> or a <b>gentle smirk</b> , indicating moments of acknowledgment or engagement in conversation. His actions, like <b>looking around and nodding</b> , suggest curiosity and agreement, while <b>talking and winking</b> reveal a playful and sociable side. These visual cues hint that he could be discussing a variety of subjects, potentially sharing insights or experiences related to personal growth, professional endeavors, or even leisure activities like movies or sports, all while maintaining an approachable and thoughtful demeanor.
Qwen3-VL-8B-Face	Judging from the background with books and the word "RED" (possibly related to a project or brand), the protagonist might be discussing topics such as his new movie, personal brand, or a motivational speech. His expressive facial movements and formal attire suggest he is engaged in a professional or promotional conversation, probably sharing insights about his career, upcoming projects, or life philosophy.
GPT-4o	The protagonist appears to be engaged in a conversation or delivering a speech. His facial expressions <b>range from serious to smiling</b> , suggesting that the topic might be light-hearted or positive at times. The setting, which includes a bookshelf, indicates that the discussion could be related to literature, education, or perhaps a casual interview. The presence of the word "RED" in the background might imply that the setting is related to a brand or a specific program that uses red as a part of its visual identity. Without audio or additional context, it's challenging to determine the exact subject of the discussion, but it seems to be a friendly and possibly informative exchange.
Qwen3-VL-30B-A3B	The protagonist in the video frames appears to be engaged in a <b>serious</b> and possibly motivational or informative discussion. The setting, with bookshelves in the background, suggests an intellectual or professional environment, which could indicate that the topic is related to knowledge, learning, or expertise. The protagonist's attire, a suit, further supports the idea that the discussion might be formal or business-related. Given these visual cues, it is likely that the protagonist is discussing themes such as personal development, career advice, or sharing insights on a specific subject matter. The consistent and focused expression of the protagonist implies that the content of the discussion is significant and intended to engage the audience's attention.

Table 13. We randomly sample multiple qualitative comparison cases (3/4) and add additional color labeling to the content involving fine-grained facial features.



Question	Please analyze the content of the video.
FaVChat	The young woman in the video exhibits a <b>clear complexion</b> with a <b>smooth texture</b> , though there are <b>slight bags</b> under her eyes that hint at potential tiredness. Her <b>long, straight brown hair</b> frames her face, enhancing her <b>youthful appearance</b> . She has a <b>neutral gaze</b> , with eyes that do not distinctly show their color but convey a <b>calm and composed look</b> . Her <b>nose is straight and well-proportioned</b> , contributing to a balanced facial structure. Her facial expressions are subtle, with no strong emotional indicators, which aligns with her overall <b>neutral demeanor</b> . She <b>accessorizes with sunglasses</b> placed atop her head, adding a <b>casual flair</b> to her appearance, and she <b>wears small hoop earrings</b> that subtly complement her features. Her <b>neutral expression</b> , combined with her physical attributes, portrays a <b>composed and approachable individual</b> , likely engaged in a casual yet reflective conversation amidst a lively outdoor setting, where other people and event structures can be seen in the background, suggesting a public or social gathering.
Qwen3-VL-8B-Face	This video features a woman being interviewed outdoors, likely in a public or recreational area with trees and other people in the background. <b>She has sunglasses on her head, wears a small necklace, and carries a camera strap</b> , suggesting she might be engaged in activities like photography or exploring.
GPT-4o	The video show a young woman with <b>long brown hair and a pair of sunglasses</b> resting on her head. She appears to be in an outdoor setting, possibly at a public event, as suggested by the presence of other people in the background and what looks like a stage or booth with equipment. The woman is wearing a green top and has a black bag slung over her shoulder. Her facial expressions vary across the frames, indicating she might be in the middle of a conversation or reacting to something happening off-camera. The logo in the corner suggests that the video may be from a channel or series named "EASY GRILL," which could imply an interview or street-style content format. There are no discernible texts or other specific details that provide context for the conversation or the event.
Qwen3-VL-30B-A3B	The video appears to show a <b>young woman with long brown hair, wearing a black top</b> , standing outdoors. She is <b>looking around</b> and seems to be engaged in a conversation or reacting to something off-camera. In the background, there are other people, including a man in a red shirt who is also looking around. The setting suggests a casual, possibly social environment, with trees and greenery visible, indicating it might be a park or an outdoor event. The woman's expressions change slightly across the frames, suggesting she is actively participating in the interaction.

Table 14. We randomly sample multiple qualitative comparison cases (4/4) and add additional color labeling to the content involving fine-grained facial features.



Question	Please analyze the identity of the protagonist in the video.
FaVChat	The character appears to be a figure of wisdom and experience with a <b>long white beard and mustache</b> , as suggested by his <b>oval face shape</b> which is traditionally associated with such qualities. His <b>baldness</b> adds a sense of maturity and might imply a high-ranking or spiritual role. The <b>bushy eyebrows and pointy nose structure</b> contribute to an intense and distinguished look, possibly indicating a character of authority or decisiveness. The <b>goatee and mustache frame his face</b> , enhancing his mature appearance and potentially emphasizing his emotional state or thoughts. His <b>well-kept skin</b> suggests self-care and maintenance, aligning with the perception of wisdom and experience. The <b>neutral expression, with a calm gaze</b> , might suggest contemplation or introspection, inviting viewers to consider the character's internal narrative. The subtle microexpressions, <b>especially around the eyes or mouth, could hint at thoughtfulness or concern</b> . Considering the traditional attire and the dignified presence, it is reasonable to infer that the protagonist could be a sage, a high-ranking official, or a respected elder within the narrative.
Qwen3-VL-8B-Face	The video shows a character who appears to be from a historical drama or film. The character is dressed in traditional Chinese attire, which suggests that the video might be set in a historical period of China. The specific identity of the protagonist cannot be determined from the video alone without additional context or information about the video's plot, setting, or production details. If you have more information or a specific question about the video, feel free to share, and I can provide further assistance.
GPT-4o	The protagonist is an elderly monk, identifiable by his <b>bald head, long white beard and eyebrows</b> , and traditional monk robes. His appearance and the context from the subtitles suggest he is a wise, possibly powerful figure in a martial arts or fantasy narrative, likely playing an important role in the plot, perhaps related to some secret or mission involving elements like "Shen Du" and another character referred to as "Zhu Que Lord".
Qwen3-VL-30B-A3B	The protagonist in the video appears to be an elderly man with a <b>long white beard and mustache</b> , wearing traditional Chinese attire. His appearance suggests that he might be a character from a historical or fantasy drama, possibly portraying a wise elder, scholar, or martial arts master. The setting and his clothing indicate a connection to ancient Chinese culture, and his demeanor conveys a sense of authority and wisdom.